Supplementary Information

Wittig olefination "baking powder": a hexameric halogen-bonded phosphonium salt cage for encapsulation and mechanochemical transformation of small-molecule carbonyl compounds

Joseph M. Marrett, Hatem M. Titi and Tomislav Friščić*

Department of Chemistry, McGill University, 801 Sherbrooke St. West, Montreal, Quebec H3A 0B8, Canada

Table of Contents

S.1. Materials **1**

S.2. Synthetic methods **1**

S.3. Electrostatic surface potential calculation methods **6**

S.4. Instrumental methods **6**

S.5. Powder X-ray diffraction data **10**

S.6. Infrared spectroscopy **17**

S.7. Thermogravimetric analysis **19**

S.8. Number of guest molecules per cage as determined by TGA and NMR **21**

S.9. Analysis of organic products **22**

S.10. ^{1}H NMR quantitative methods **24**

S.11. Raw ^{1}H NMR of cage materials **25**

S.12. Raw ^{1}H NMR of crude Wittig olefination reaction milling products **35**

S.13. Raw ^{1}H and ^{13}C NMR of purified products **38**

S.14. References **46**

S1. Materials

Carbon tetrabromide (99%), acetaldehyde (≥99%), acrylic acid (99%), dimethylacetamide (DMA) (≥99%), nitromethane ($MeNO_2$) (≥95%), N-methyl-2-pyrrolidone (NMP) (99%), nitrobenzene (99%), cyclohexanone (99.8%), iodoform (99%), benzene (anhydrous, 99.8%), carbon tetrachloride (99.9%) and copper(I) iodide (≥99.5%) were obtained from Sigma Aldrich. Triphenylphosphine (99%), cyclohex-2-enone (98%), propionaldehyde (97%), isobutyraldehyde (99%), butyraldehyde (96%), 3-(methylthio)propionaldehyde (methional) (97%), cyclobutanone (≥98%), diethyl propionamide (≥95%), (trimethylsilyl)acetylene (98%) and 1,1'-bis(diphenylphosphino)ferrocene-palladium(II) dichloride dichloromethane complex (98%) were obtained from Oakwood Chemical. Dimethyl sulfoxide (DMSO) (99.9%), dimethyl formamide (DMF) (99.8%), acetic acid (99.5%), and potassium carbonate (99%) were obtained from ACP Chemicals. Butanone (99.9%), and acetone (99.5%) were obtained from Fischer chemical. All chemicals were used without purification, except benzene which was stored over molecular sieves and subject to three cycles of freeze-pump-thaw degassing under argon before use in solution experiments.

S2. Synthetic methods

S2.1. Synthesis of (dibromomethyl)triphenylphosphonium bromide (1)

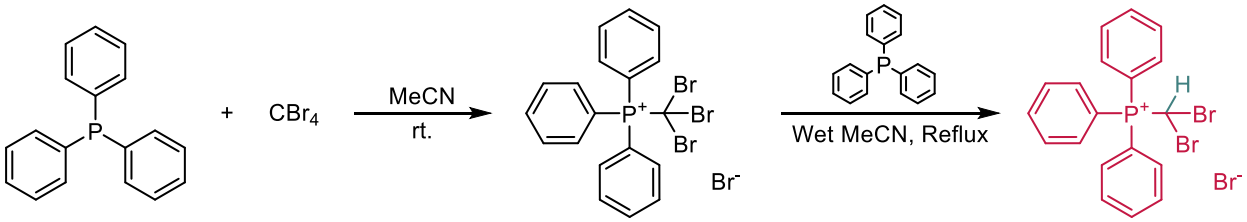

Scheme 1. Reaction scheme for the synthesis of **1**.

Compound **1** was synthesized according to a procedure previously reported by Wolkoff.[1] The general scheme for this reaction is shown above. The product of this synthesis is microcrystalline **1•MeCN** which can be recrystallized carefully from MeCN to yield crystals suitable for single crystal x-ray diffraction analysis (scXRD). Yield for step 1: 84 %. Yield for second step: 44%.

S2.2. Desolvation of 1•MeCN to form desolvated 1

Microcrystalline **1•MeCN** was exposed to 130 °C under high vacuum for 14 hours to yield desolvated **1.** Recrystallization of this powder by slow cooling from nitrobenzene produces single crystals suitable for scXRD analysis which revealed the structure of solvent-free **1**.

S2.3. Procedure for synthesis of 1•guest materials

Materials of the type **1•guest** were formed by recrystallization of **1** from hot liquid **guest** followed by collection by filtration. In the case of materials grown from non-volatile liquids (NMP, DMF, DMA, acetic acid, acrylic acid, DMSO, cyclohexanone, cyclohex-2-enone), the solid product is rinsed with benzene during the filtration step before drying on the frit

for 5 minutes. In the case of cyclohexanone and cyclohex-2-eneone, precipitation of the cage material is particularly slow (~48 hrs) and was carried out in the freezer (-18 °C). In the cases where single crystal structures were collected, suitable crystals were collected from the mother liquor by pipette before filtration.

S2.4. Procedure for the synthesis of 1•reactive-guest materials

Bulk powders of the **1•reactive-guest** materials used in all milling experiments were obtained by soaking 200 mg (0.39 mmol) of **1** in 1 mL of the liquid guest for 24 hours followed by filtration and washing with benzene. Single crystals of **1•acetaldehyde** were grown by recrystallization of **1** from a hot mixture of 50 v/v% acetaldehyde in nitrobenzene. Single crystals of **1•propionaldehyde** are grown in the same fashion from a 50 v/v% mixture of propionaldehyde in N,N-diethylpropionamide. Single crystals of **1•butyraldehyde** and **1•isobutyraldehyde** were obtained by adding a very small amount (~5 mg) of **1** to a large excess (1 mL) of liquid aldehyde and letting the powder soak for 24 hours to yield single crystals. X-ray quality single crystals **1•cyclobutanone** could be obtained by simple recrystallization of **1** from the hot liquid cyclobutanone.

S2.5. Procedure for the synthesis of reactive 1•guest materials by milling

Bulk powders of the **1•reactive-guest** materials can also be obtained by ball-milling **1** with the guest liquid. 100 mg (0.19 mmol) of **1** and 100 µL of the liquid guest are added to a 15 mL zirconia milling jar with a single zirconia ball of 3.2 g weight. The mixture is milled for 5 to 30 minutes (see PXRD data for specific times) at 30 Hz using a Form-Tech Scientific FTS-1000 shaker mill.

S2.6. General procedure for the mechanochemical Wittig olefination *via* 1•guest

90 mg of **1•reactive-guest** and 1.1 equivalents of K_2CO_3 (between 22.1mg and 24.5 mg depending on the guest loadings as determined by ^{1}H NMR, as shown in Table S.6.) are added to a 15 mL zirconia milling jar with a single 3.2 g zirconia ball, and the mixture is milled for 30 minutes at 25 Hz. Analysis proceeds immediately by ^{1}H NMR spectroscopy in $CDCl_3$. Yields were determined by ^{1}H NMR as explained in **S10.2.** The *gem*-dibromoolefin product was purified either by distillation from the solid reaction mixture or column chromatography; specifics for each sample are listed in section **S9.**

S2.7. Procedure for the one-pot mechanochemical combination of Wittig olefination and Sonogashira coupling using 1•guest as the starting material

In a typical experiment, 90 mg of **1•reactive-guest** material is added to a 15 mL zirconia milling jar with one 3.2 g zirconia ball. 10 mol % $PdCl_2(dppf)\cdot CH_2Cl_2$, 8 mol % CuI, potassium carbonate, and (trimethylsilyl)acetylene are added and the mixture is milled at 30 Hz. The required mass of catalyst was calculated based on the quantity of guest assuming a loading of 5 molecules per cage. The temperature of the reaction mixtures immediately after milling were measured using an infrared thermometer and were found to never exceed 29 °C. Chemical analysis proceeds immediately by ^{1}H NMR spectroscopy in $CDCl_3$. Conversions were determined by ^{1}H NMR as explained in **S10.3.** Purification of the product(s) proceeds by column chromatography of the jar contents; specifics for each product are listed in **S9.**

S2.8. Procedure for attempted one-pot combination of Wittig olefination and Sonogashira coupling in solution

For each experiment, 90 mg of **1•butyraldehyde**, 2 mL of anhydrous benzene degassed by three freeze-pump-thaw cycles under argon, a base, $PdCl_2$(**dppf)** (10 mol %), CuI (8 mol %), and (trimethylsilyl)acetylene (3.3 eq.) were added to a sealed, oven-dried vial and stirred under argon for the time indicated in Table S2.1. Reactions using diisopropylethylamine mimic conditions used by Uenishi *et al.* for the coupling of terminal acetylenes with 1,1-dibromoolefins.[2] Workup for all reactions involved the removal of solvent *in vacuuo* before ^{1}H NMR analysis of the crude product mixtures. Conversions were determined by ^{1}H NMR as explained in **S10.3.**

Table S2.1. Conditions and conversions for attempted one-pot combination of Wittig olefination and Sonogashira coupling.

Base	Reaction time	Reaction temperature	Wittig product	Sonogashira coupling products
2.5 eq. K_2CO_3	90 min	room temperature	yes	none
2.5 eq. K_2CO_3 sesquihydrate	90 min	room temperature	yes	none
2.5 eq. K_2CO_3	24 hours	room temperature	yes	none
2.5 eq. K_2CO_3 sesquihydrate	24 hours	room temperature	no	eneyne: 17% enediyne: 8%
2.5 eq. K_2CO_3	90 min	40 °C	yes	none
2.5 eq. K_2CO_3 sesquihydrate	90 min	40 °C	yes	none
2.5 eq. K_2CO_3	24 hours	40 °C	yes	none
2.5 eq. K_2CO_3 sesquihydrate	24 hours	40 °C	none	eneyne: < 5% enediyne: 14%
4 eq. *i*-Pr_2NH See Ref.[2]	90 min	room temperature	Yes	none
4 eq. *i*-Pr_2NH See Ref.[2]	90 min	40 °C	yes	none
4 eq. *i*-Pr_2NH See Ref.[2]	24 hours	room temperature	yes	eneyne: 9% enediyne: none
4 eq. *i*-Pr_2NH See Ref.[2]	24 hours	40 °C	yes	eneyne: 7% enediyne: none

S2.9. Procedure for attempted solution-based Sonogashira coupling from pre-synthesized 1,1-dibromopentene

To an oven-dried vial were added 30 mg (0.13 mmol) 1,1-dibromopentene, $PdCl_2$(**dppf**) (10 mol %), CuI (8 mol %), (trimethylsilyl)acetylene (3.3 eq), and 2 mL of degassed anhydrous benzene. As a base were used either 1.5 equivalents K_2CO_3 sesquihydrate or 3 equivalents of diisopropylamine.[2] The reaction vial was sealed and the reaction mixture stirred under argon for the time indicated in Table S2.2. Conversions were determined by comparing ^{1}H NMR integration of signals of the dibromide starting material and the signals of the eneyne and enediyne products.

Table S2.2. Conditions and conversions for solution-based Sonogashira reactions of 1,1-dibromopentene.

Base	Reaction time	Reaction temperature	Remaining starting material (1,1-dibromopentene)	eneyne conversion	enediyne conversion
1.5 eq. K_2CO_3	90 min	room temperature	100%	none	none
1.5 eq. K_2CO_3 sesquihydrate	24 hours	room temperature	50%	39%	11%
3 eq. *i*-Pr_2NH See Ref.[2]	90 min	room temperature	none	79%	21%
3 eq. *i*-Pr_2NH See Ref.[2]	24 hours	room temperature	none	none	100%

S2.10. Procedure for the synthesis of (dichloromethyl)triphenylphosphonium chloride (2)

The salt **2** was synthesized according to a modified procedure reported by Appel *et al*,[3] scaled down 100-fold. 2 mL (20.7 mmol) of CCl_4 and 524 mg (2 mmol) of triphenylphosphine were added to a mixture of 4.2 mL benzene and 0.8 mL acetonitrile. The mixture was heated to 50 °C in a sealed vial with rapid stirring. After 5 minutes, the mixture turned a pale yellow, and the vial was opened to the air with continued stirring. After 10 minutes, a white precipitate formed which was isolated by filtration and washed with a minimal amount of benzene. Crystals for scXRD structural analysis were obtained by slow evaporation of a solution of this material in MeCN. Yield: 55%.

S2.11. Procedure for the synthesis of (diiodomethyl)triphenylphosphonium iodide (3) and (iodomethyl)triphenylphosphonium iodide (4)

1.18 g (3 mmol) of iodoform and 787 mg (3 mmol) of triphenylphosphine were added to 5 ml of MeCN and dissolved fully by sonication. The mixture was refluxed for 5 minutes, until a deep red paste formed on the walls of the vessel. This paste was broken up using a glass rod and by submersion of the sealed vessel in a sonicating bath, converting it to a yellow powder in the process. This powder was collected by filtration was suspended in 10 mL of acetonitrile and again collected by filtration before drying briefly on the frit. After collection, the product was stored under an inert atmosphere. Single crystals of **3•MeNO$_2$** were grown by evaporation of a solution made by dissolving this powder in $MeNO_2$ under high vacuum over the course of approximately 20 minutes. Longer evaporation times, or the use of elevated temperature produced single crystals of

(iodomethyl)triphenylphosphonium iodide (**4**) whose crystal structure is also reported here.

S3. Electrostatic surface potential (ESP) calculations

Electrostatic surface potential maps were calculated for the cations of salts **1**, **2**, and **3**, based on their structures after geometry optimization using Gaussian 16[4] at the B3LYP/cc-pVTZ level of theory.[5] The basis set aug-cc-pVTZ was used for the iodine atoms of **3**, and was sourced from the basis set exchange.[6] ESPs were visualized in Vesta.[7]

S4. Instrumental methods

S4.1. Nuclear magnetic resonance spectroscopy (NMR)

Solution ^{1}H and ^{13}C nuclear magnetic resonance spectra were collected using either a Varian Inova 500 MHz spectrometer operating at 500 MHz for ^{1}H nuclei and 125 MHz for ^{13}C nuclei or a Varian VNMRS 500 MHz spectrometer operating at the same frequencies. Chemical shifts are reported relative to $CDCl_3$ (δ = 7.26 ppm for ^{1}H; δ = 77.16 ppm for ^{13}C).

S4.2. Mass spectrometry (MS)

GCMS data was obtained using a Bruker Scion single quadropole GC/MS. APCI-MS data was obtained using a Bruker Maxis Impact API QqTOF spectrometer.

S4.3. Thermogravimetric Analysis (TGA)

Thermogravimetric analysis was performed using a Mettler Toledo TGA/DSC 1 instrument. The samples (approximately 10 mg each) were placed in 70 µL open-top alumina crucibles and measurments were conducted under a stream of nitrogen gas (50 ml min^{-1}) from room temprature to 200 °C at a rate of 10 °C min^{-1}.

S4.4. Powder x-ray diffraction (PXRD)

Powder X-ray diffraction data was collected using a Bruker D2 PHASER difractometer which was outfitted with a LynxEye liner position-sensitive detector using nickel-filtered CuK_α X-ray radiation.

S4.5. Single crystal X-ray crystal structure determination

Single crystal X-ray diffraction (scXRD) data were measured on a Bruker D8 Venture diffractometer equipped with a Photon 200 area detector, and *IµS* microfocus X-ray source (Bruker AXS, Cu*K*α source). Measurements were carried out at 180(2) K for **1**, **1·MeNO$_2$**, **1·acetic acid**, and **1·acrylic acid**, and 153(2) K for **1·DMA,** while the rest were mounted at 298(2) K. Crystals were coated with a thin layer of paratone oil before mounting on the diffractometer. Structure solution was carried out using the SHELXTL package.[8] The parameters were refined for all data by full-matrix-least-squares refinement of F^2 using SHELXL.[9] The structures **1·MeCN**, **1·acetone**, **1·2-butanone**, **1·acetic acid**, **1·DMSO**, **1·acetaldehdye**, and **1·cyclobutanone** exhibit disordered

moieties that were modeled successfully. Due to the large thermal motion in **1·MeCN,** the atoms of the included guest molecules were modeled isotropically. The crystal structure of compound **4** was determined from a single crystal that was found to be twinned by inversion. Crystalline compounds **1·MeCN**, **1·MeNO$_2$**, **1·acetone**, **1·acetic acid**, **1·acrylic acid**, **1·DMSO**, **1·NMP**, **1·DMF**, **1·isobutyraldehyde**, and **1·propionaldehyde** contain disordered guest molecules that are positioned on a 3-fold screw axis, and therefore were challenging to model. The electron density corresponding to these symmetry-disordered guests were subtracted using the SQUEEZE procedure, as included in the PLATON software package.[10] All of the non-hydrogen atoms were refined with anisotropic thermal parameters, and the coordinates of all hydrogen atoms were constrained to ride on their carrier atom.

Crystallographic data in CIF format for all herein determined crystal structures can be accessed using the joint CCDC/FIZ Karlsruhe online deposition service (www.ccdc.cam.ac.uk/structures/), under the deposition numbers 2095086-2095103.

Table S4.1. Crystallographic data for herein determined single crystal structures.

Compound	1	1·MeCN	1·$MeNO_2$	1·acetone	1·2-butanone	1·acetic acid	1·acrylic acid	1·DMSO	1·NMP	1·DMF
Empirical formula	$C_{19}H_{16}Br_3P$	$C_{21}H_{19}Br_3NP$	$C_{20}H_{19}Br_3NO_2P$	$C_{22}H_{22}Br_3OP$	$C_{23}H_{24}Br_3OP$	$C_{21}H_{20}Br_3O_2P$	$C_{22}H_{20}Br_3O_2P$	$C_{21}H_{22}Br_3OPS$	$C_{24}H_{25}Br_3NOP$	$C_{22}H_{23}Br_3NOP$
M_r	515.02	556.07	576.06	573.09	587.12	575.07	587.08	593.14	614.15	588.11
T/K	180(2)	298(2)	180(2)	298(2)	298(2)	180(2)	180(2)	298(2)	298(2)	298(2)
Crystal system	monoclinic	trigonal	trigonal	trigonal	trigonal	trigonal	trigonal	trigonal	trigonal	trigonal
Space group	*C*2/c	*R*-3	*R*-3	*R*-3	*R*-3	*R*-3	R-3	*R*-3	*R*-3	*R*-3
a/Å	17.7546(4)	33.1499(5)	32.270(2)	33.0003(6)	33.4263(4)	32.4936(8)	32.283(2)	33.4643(5)	33.612(2)	33.1823(9)
b/Å	15.5320(3)	33.1499(5)	32.270(2)	33.0003(6)	33.4263(4)	32.4936(8)	32.283(2)	33.4643(5)	33.612(2)	33.1823(9)
c/Å	28.3321(6)	11.1629(2)	11.3230(8)	11.1350(2)	11.2099(2)	11.3322(8)	11.5522(8)	11.1613(2)	11.4292(7)	11.4506(3)
α/°	90	90	90	90	90	90	90	90	90	90
β/°	99.228(1)	90	90	90	90	90	90	90	90	90
γ/°	90	120	120	120	120	120	120	120	120	120
V/Å^3	7711.9(3)	10623.6(4)	10211.4(15)	10501.6(4)	10847.0(3)	10361.9(9)	10426.7(15)	10824.5(4)	11182.4(17)	10918.7(7)
Z	16	18	18	18	18	18	18	18	18	18
ρ_{calc}/g cm^{-3}	1.774	1.565	1.686	1.631	1.618	1.659	1.683	1.638	1.642	1.610
μ/mm^{-1}	8.506	7.007	7.381	7.126	6.914	7.259	7.230	7.725	6.750	6.883
F(000)	4000.0	4896.0	5076.0	5076.0	5220.0	5076.0	5184.0	5256.0	5472.0	5220.0
2θ range for data collection/°	6.32 to 144.588	8.498 to 144.72	8.426 to 145.472	8.522 to 144.792	8.458 to 144.352	10.89 to 144.722	8.282 to 145.226	11.318 to 144.396	5.258 to 144.34	5.326 to 145.218
Index ranges	-21 ≤ h ≤ 20, -12 ≤ k ≤ 19, -34 ≤ l ≤ 34	-40 ≤ h ≤ 40, -40 ≤ k ≤ 40, -13 ≤ l ≤ 5	-39 ≤ h ≤ 39, -39 ≤ k ≤ 31, -11 ≤ l ≤ 14	-40 ≤ h ≤ 40, -40 ≤ k ≤ 40, -13 ≤ l ≤ 8	-31 ≤ h ≤ 41, -41 ≤ k ≤ 30, -8 ≤ l ≤ 13	-40 ≤ h ≤ 40, -40 ≤ k ≤ 40, -13 ≤ l ≤ 9	-28 ≤ h ≤ 39, -39 ≤ k ≤ 37, -14 ≤ l ≤ 11	-41 ≤ h ≤ 41, -40 ≤ k ≤ 41, -8 ≤ l ≤ 13	-41 ≤ h ≤ 41, -41 ≤ k ≤ 41, -14 ≤ l ≤ 11	-40 ≤ h ≤ 40, -40 ≤ k ≤ 40, -10 ≤ l ≤ 14
Reflections collected	67258	25997	17041	58815	20559	26076	20408	61014	76439	74379
Independent reflections	7620 [R_{int} = 0.0643, R_{sigma} = 0.0295]	4593 [R_{int} = 0.0364, R_{sigma} = 0.0284]	4416 [R_{int} = 0.0366, R_{sigma} = 0.0330]	4613 [R_{int} = 0.0416, R_{sigma} = 0.0167]	4617 [R_{int} = 0.0312, R_{sigma} = 0.0254]	4448 [R_{int} = 0.0306, R_{sigma} = 0.0226]	4593 [R_{int} = 0.0539, R_{sigma} = 0.0439]	4702 [R_{int} = 0.0371, R_{sigma} = 0.0183]	4907 [R_{int} = 0.0943, R_{sigma} = 0.0277]	4798 [R_{int} = 0.0540, R_{sigma} = 0.0203]
Data /restraints /parameters	7620/54/415	4593/42/230	4416/18/245	4613/253/263	4617/222/266	4448/280/275	4593/0/254	4702/309/263	4907/18/272	4798/338/255
S	1.029	1.064	1.042	1.083	1.077	1.041	1.054	1.065	1.086	1.056
Final R values ($I \geq 2\sigma_I$)	R_1 = 0.0328, wR_2 = 0.0806	R_1 = 0.0372, wR_2 = 0.0977	R_1 = 0.0278, wR_2 = 0.0647	R_1 = 0.0291, wR_2 = 0.0655	R_1 = 0.0291, wR_2 = 0.0700	R_1 = 0.0336, wR_2 = 0.0880	R_1 = 0.0411, wR_2 = 0.0957	R_1 = 0.0393, wR_2 = 0.1037	R_1 = 0.0419, wR_2 = 0.1021	R_1 = 0.0445, wR_2 = 0.1179
Final R values [all data]	R_1 = 0.043, wR_2 = 0.088	R_1 = 0.041, wR_2 = 0.101	R_1 = 0.031, wR_2 = 0.067	R_1 = 0.036, wR_2 = 0.071	R_1 = 0.032, wR_2 = 0.072	R_1 = 0.036, wR_2 = 0.090	R_1 = 0.046, wR_2 = 0.010	R_1 = 0.041, wR_2 = 0.106	R_1 = 0.074, wR_2 = 0.137	R_1 = 0.055, wR_2 = 0.132
Largest diff. peak/hole / e Å^{-3}	0.69/-0.47	0.69/-0.54	0.47/-0.64	1.44/-0.44	0.41/-0.52	0.99/-0.66	2.95/-0.78	1.20/-0.81	0.39/-0.63	0.65/-0.66

Table S4.2. Crystallographic data for herein determined single crystal structures.

Compound	1·DMA	1·acetaldehdye	1·isobutyraldehyde	1·cyclobutanone	1·proprionaldehyde	2	3	4
Empirical formula	$C_{23}H_{25}Br_3NOP$	$C_{21}H_{20}Br_3OP$	$C_{22}H_{22}Br_3O_{0.75}P$	$C_{23}H_{22}Br_3OP$	$C_{42}H_{41}Br_6OP_2$	$C_{19}H_{16}Cl_3P$	$C_{20}H_{19}I_3NO_2P$	$C_{19}H_{17}I_2P$
M_r	602.14	559.07	569.09	585.10	1103.15	381.64	717.03	530.09
T/K	153(2)	298(2)	298(2)	298(2)	298(2)	298(2)	298(2)	298(2)
Crystal system	trigonal	trigonal	trigonal	trigonal	trigonal	orthorhombic	trigonal	orthorhombic
Space group	*R*-3	*R*-3	*R*-3	*R*-3	*R*-3	*Pnma*	*R*-3	$Pca2_1$
a/Å	33.0726(18)	32.8339(5)	33.1440(5)	33.2157(4)	32.8602(12)	12.2883(2)	32.9862(15)	14.8074(2)
b/Å	33.0726(18)	32.8339(5)	33.1440(5)	33.2157(4)	32.8602(12)	12.5399(2)	32.9862(15)	12.4892(2)
c/Å	11.3690(6)	11.1368(2)	11.4650(2)	11.3174(2)	11.2660(4)	12.1077(2)	12.0449(8)	20.5366(3)
α/°	90	90	90	90	90	90	90	90
β/°	90	90	90	90	90	90	90	90
γ/°	120	120	120	120	120	90	120	90
V/Å^3	10769.3(13)	10397.7(4)	10907.2(4)	10813.4(3)	10535.1(9)	1865.72(5)	11350.1(13)	3797.89(10)
Z	18	18	18	18	9	4	18	8
ρ_{calc}/g cm^{-3}	1.671	1.607	1.560	1.617	1.565	1.359	1.888	1.854
μ/mm^{-1}	6.993	7.182	6.849	6.936	7.062	5.214	29.905	26.752
F(000)	5364.0	4932.0	5040.0	5184.0	4869.0	784.0	6048.0	2016.0
2θ range for data collection/°	8.368 to 144.926	9.33 to 144.818	10.676 to 144.874	9.222 to 144.97	9.322 to 144.686	10.156 to 144.696	5.358 to 144.13	7.078 to 144.93
Index ranges	-40 ≤ h ≤ 40, -40 ≤ k ≤ 40, -14 ≤ l ≤ 12	-40 ≤ h ≤ 40, -40 ≤ k ≤ 40, -13 ≤ l ≤ 13	-40 ≤ h ≤ 40, -40 ≤ k ≤ 40, -14 ≤ l ≤ 10	-41 ≤ h ≤ 40, -40 ≤ k ≤ 41, -13 ≤ l ≤ 13	-33 ≤ h ≤ 40, -40 ≤ k ≤ 40, -5 ≤ l ≤ 13	-15 ≤ h ≤ 15, -15 ≤ k ≤ 15, -14 ≤ l ≤ 14	-40 ≤ h ≤ 40, -39 ≤ k ≤ 40, -14 ≤ l ≤ 11	-16 ≤ h ≤ 18, -15 ≤ k ≤ 15, -25 ≤ l ≤ 25
Reflections collected	70134	71554	74083	71483	25610	33961	23348	76797
Independent reflections	4728 [R_{int} = 0.0379, R_{sigma} = 0.0146]	4570 [R_{int} = 0.0601, R_{sigma} = 0.0218]	4764 [R_{int} = 0.0488, R_{sigma} = 0.0198]	4760 [R_{int} = 0.0421, R_{sigma} = 0.0163]	4601 [R_{int} = 0.0644, R_{sigma} = 0.0522]	1936 [R_{int} = 0.0645, R_{sigma} = 0.0201]	4966 [R_{int} = 0.1053, R_{sigma} = 0.0679]	7463 [R_{int} = 0.0464, R_{sigma} = 0.0242]
Data /restraints /parameters	4728/12/265	4570/219/257	4764/225/254	4760/30/275	4601/221/244	1936/0/112	4966/24/248	7463/25/398
S	1.067	1.046	1.046	1.053	1.029	1.053	1.047	1.054
Final R values ($I \geq 2\sigma_I$)	R_1 = 0.030, wR_2 = 0.069	R_1 = 0.031, wR_2 = 0.091	R_1 = 0.037, wR_2 = 0.089	R_1 = 0.032, wR_2 = 0.100	R_1 = 0.055, wR_2 = 0.160	R_1 = 0.037, wR_2 = 0.083	R_1 = 0.060, wR_2 = 0.152	R_1 = 0.022, wR_2 = 0.053
Final R values (all data)	R_1 = 0.0309, wR_2 = 0.0701	R_1 = 0.0382, wR_2 = 0.0980	R_1 = 0.0420, wR_2 = 0.0945	R_1 = 0.0356, wR_2 = 0.1052	R_1 = 0.0662, wR_2 = 0.1764	R_1 = 0.0539, wR_2 = 0.1000	R_1 = 0.0976, wR_2 = 0.1826	R_1 = 0.0232, wR_2 = 0.0538
Largest diff. peak/hole / e Å^{-3}	0.70/-0.48	1.09/-0.42	0.71/-0.86	1.20/-0.57	1.61/-0.79	0.30/-0.23	3.72/-1.51	0.95/-0.75

S5. Powder X-ray diffraction data

S5.1. PXRD patterns of 1•guest materials made *via* recrystallization from solution

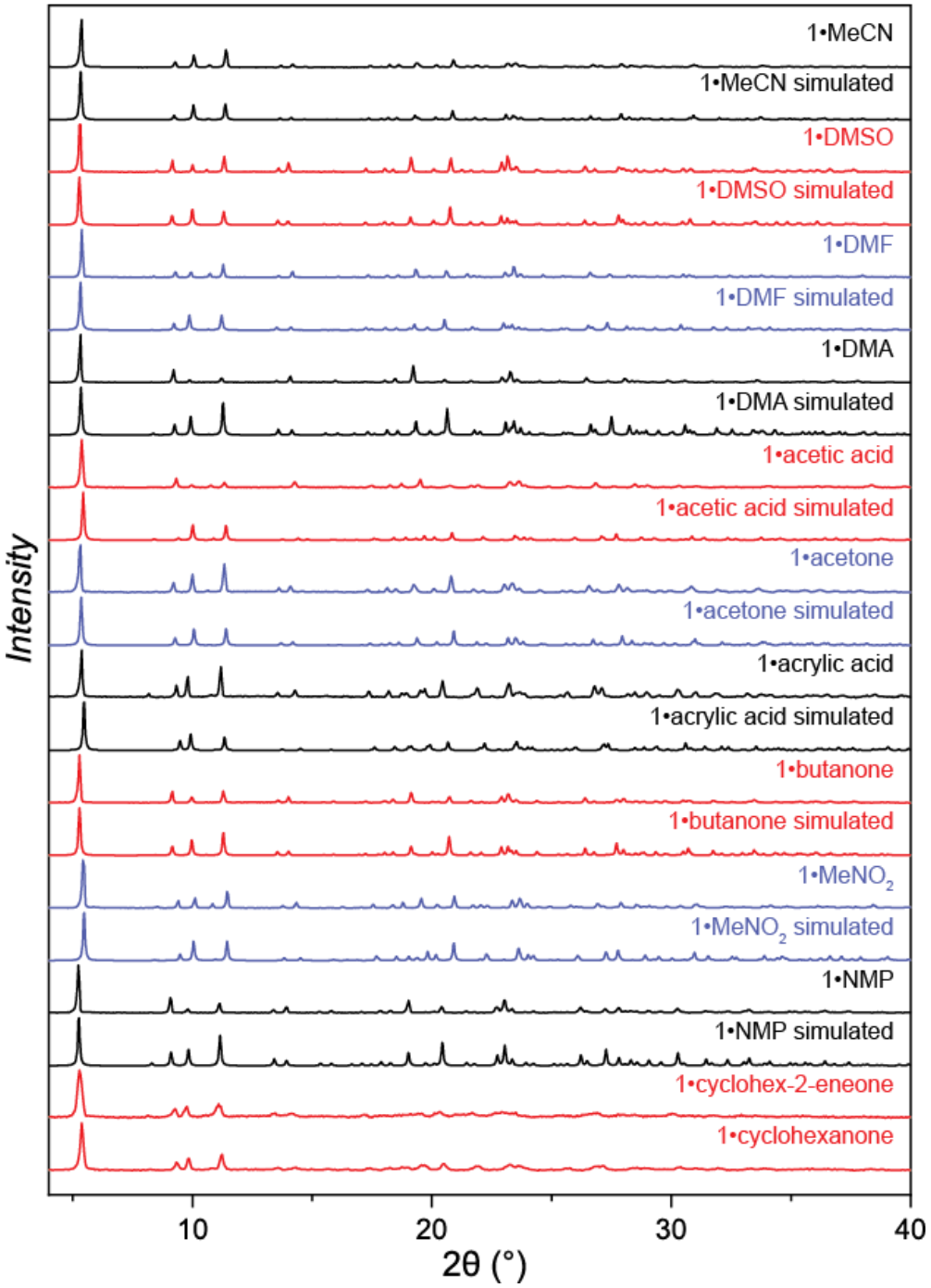

Figure S5.1. Comparisons of PXRD patterns of **1•guest** materials grown from solution. PXRD patterns simulated from scXRD crystal structures are shown for each material, if available.

S5.2. PXRD patterns of 1•reactive-guest materials made *via* soaking

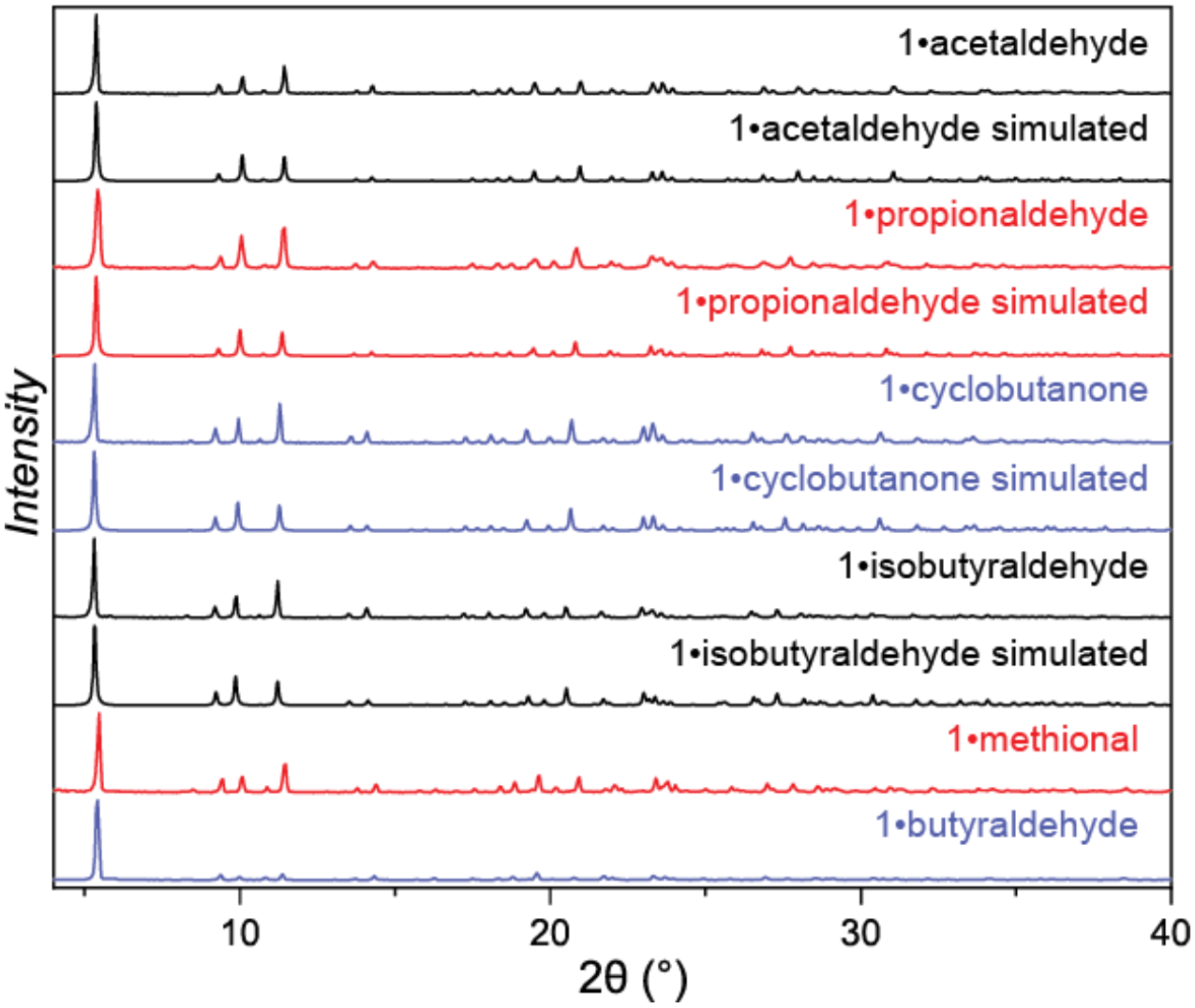

Figure S5.2. Comparisons of PXRD patterns of **1•reactive-guest** materials grown from solution. PXRD patterns simulated from scXRD crystal structures are shown for each material, if available.

S5.3. PXRD patterns of reactive 1•guest materials made *via* milling

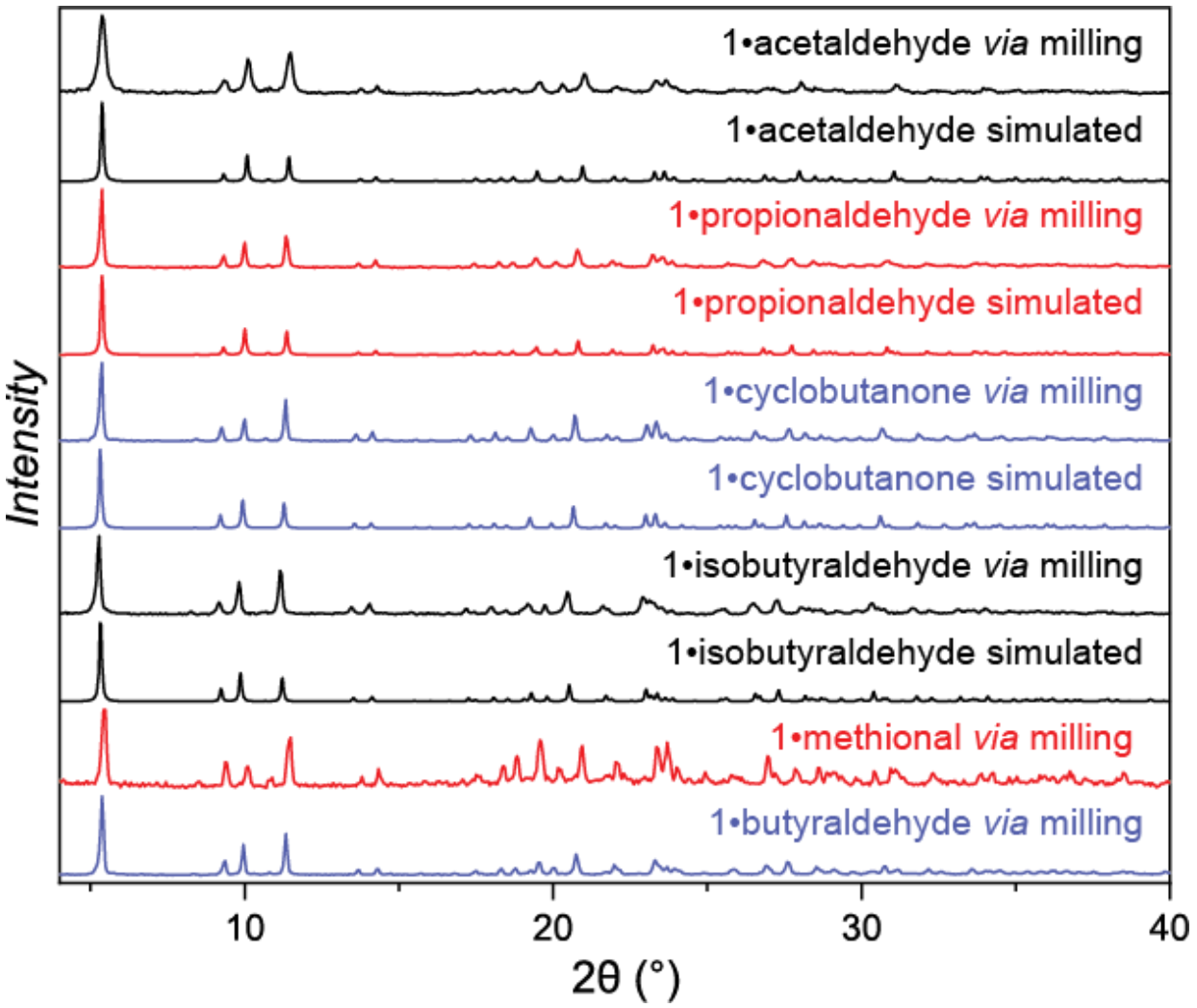

Figure S5.3. Comparisons of PXRD patterns of 1•**reactive-guest** made by milling. PXRD patterns simulated from scXRD crystal structures are shown for each material, if available.

S5.4. PXRD patterns of 1 after solvation, desolvation, and milling

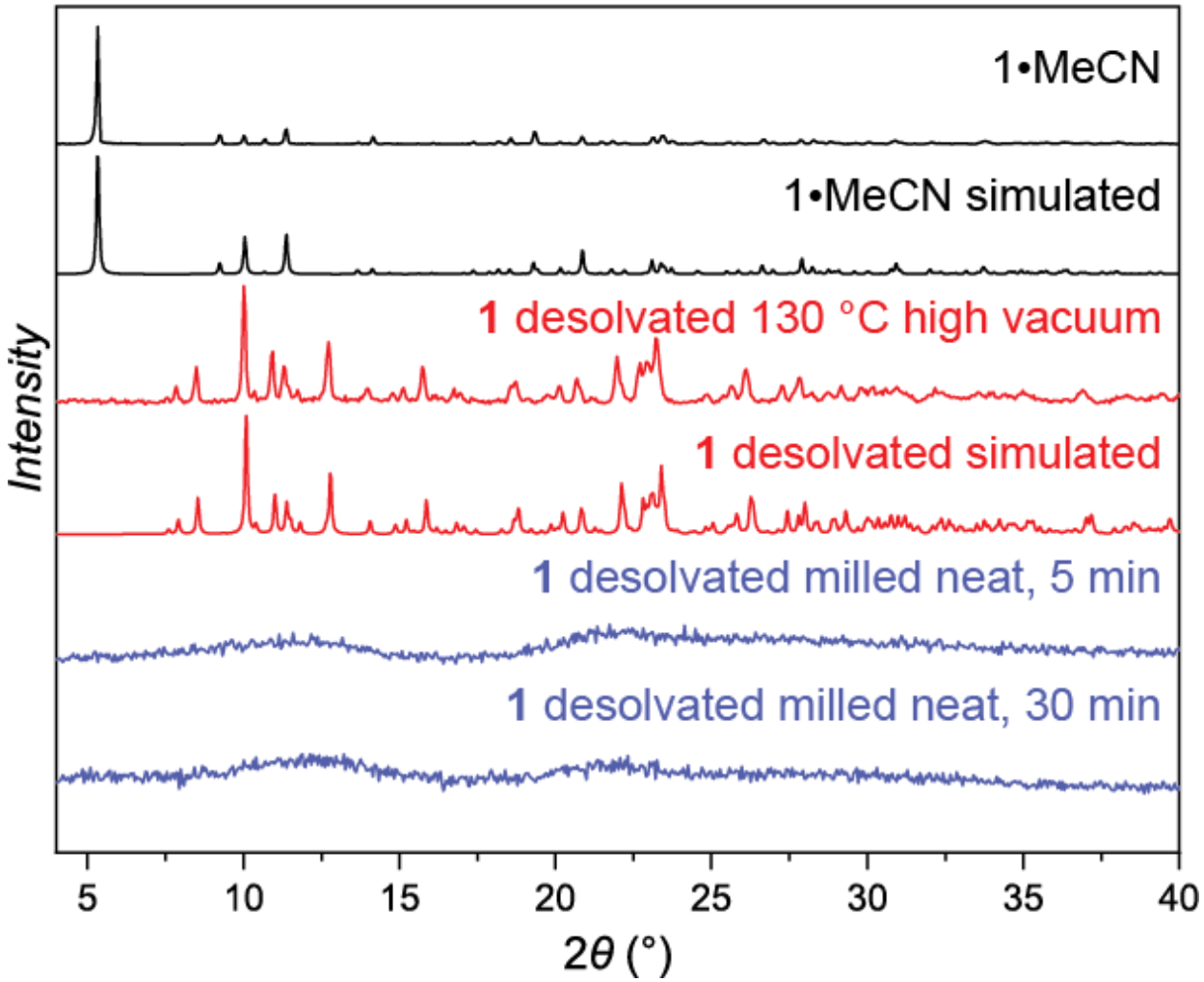

Figure S5.4. Comparisons of PXRD patterns of **1** (from top to bottom): solvated with MeCN; desolvated using heat *en vacuuo*; amorphous due to milling.

S5.5. PXRD patterns of 1•butyraldehyde and the crystalline byproducts of the Wittig olefination using 1•butyraldehyde

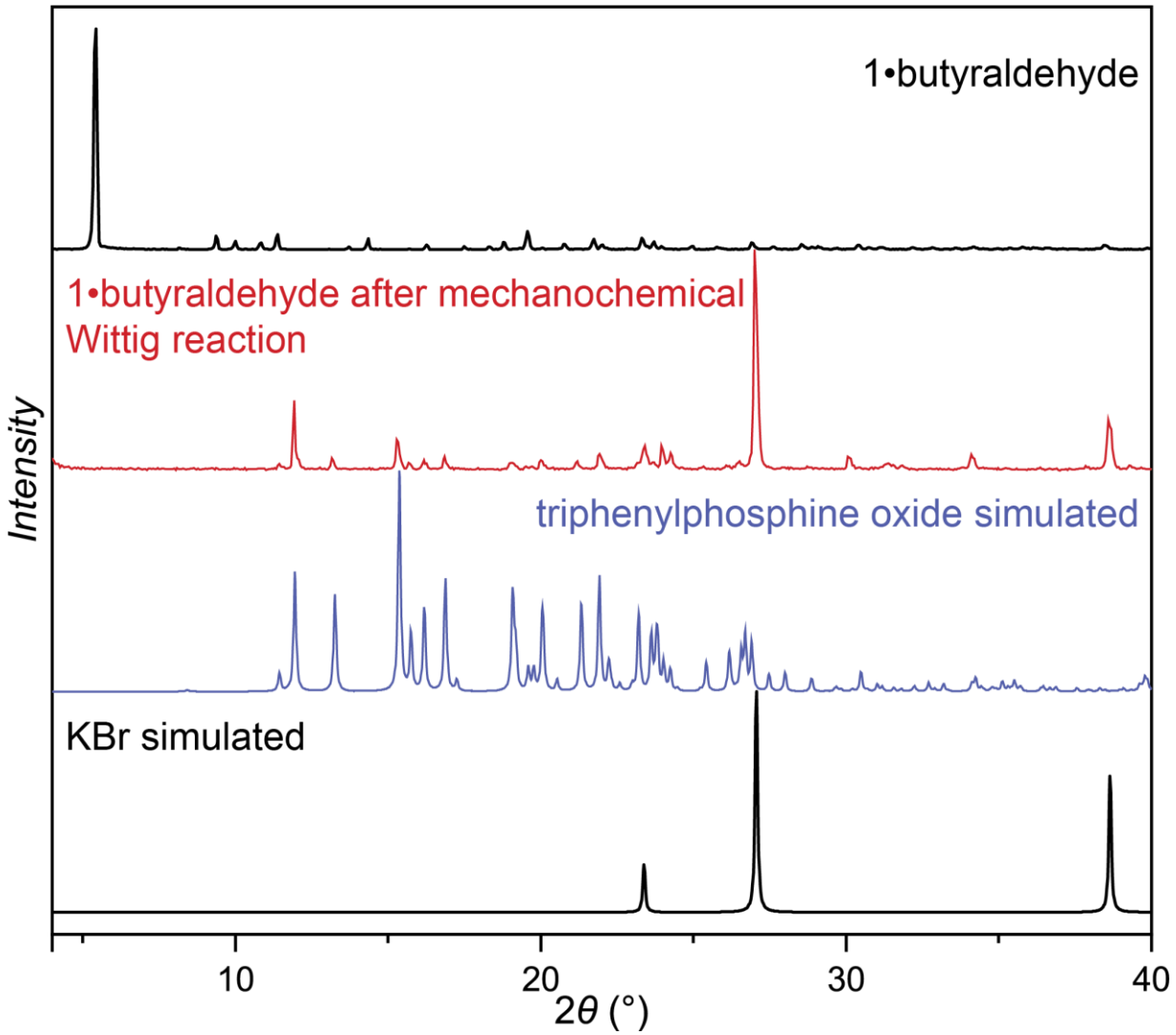

Figure S5.5. Comparison of PXRD patterns of **1•butyraldehyde** before and after Wittig olefination with potential crystalline byproducts of the reaction (from top to bottom): **1•butyraldehyde**; crude reaction product after Wittig olefination using **1•butyraldehyde**; triphenylphosphine oxide[11] simulated; KBr simulated.[12]

S5.6. PXRD patterns of selected materials in the synthesis of 2

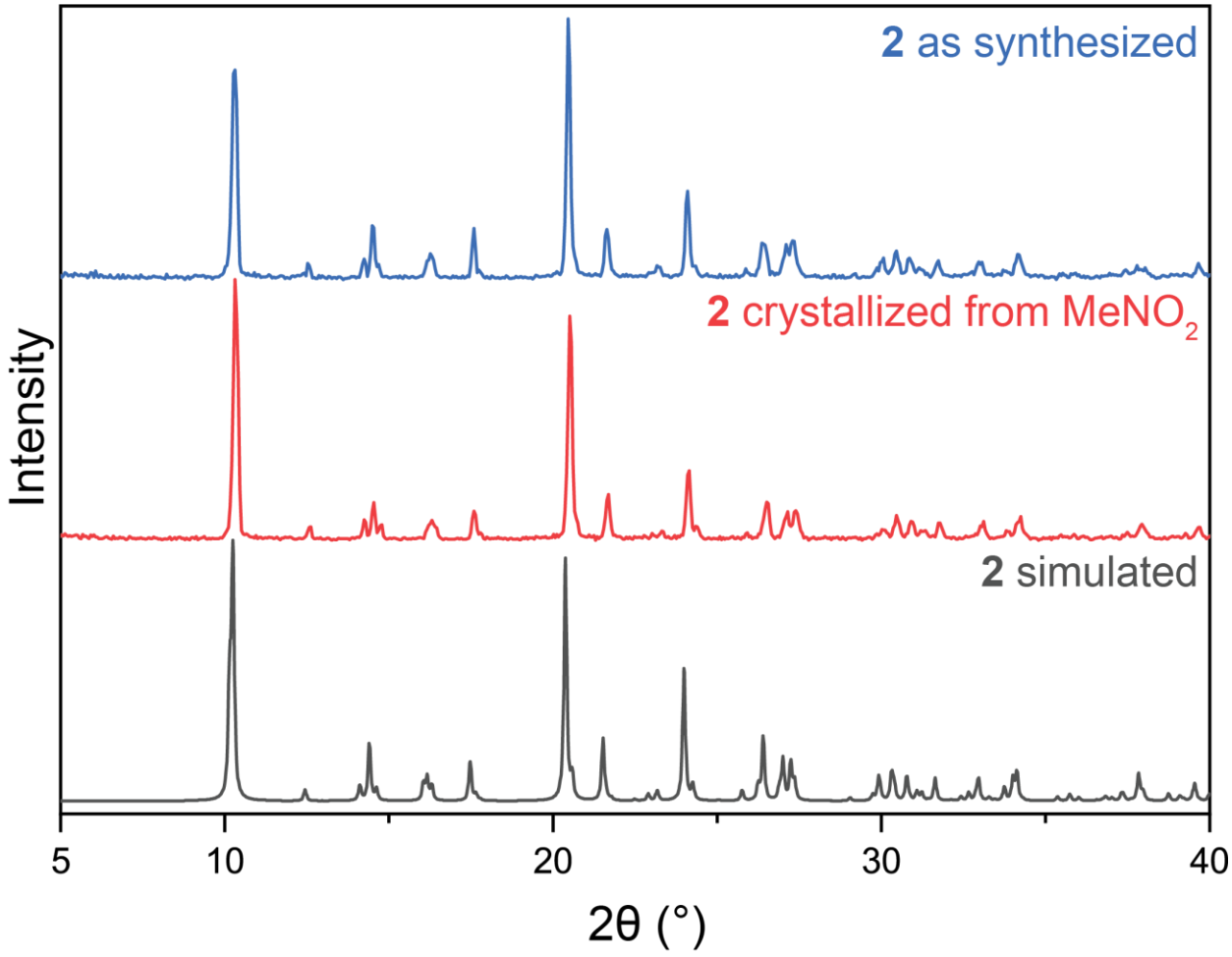

Figure S5.6. Comparison of PXRD patterns of compound **2** (from top to bottom): as-synthesized from benzene solution; after recrystallization from $MeNO_2$; and simulated for the herein determined crystal structure.

S5.7. PXRD patterns of the selected materials in the synthesis of 3 and 4

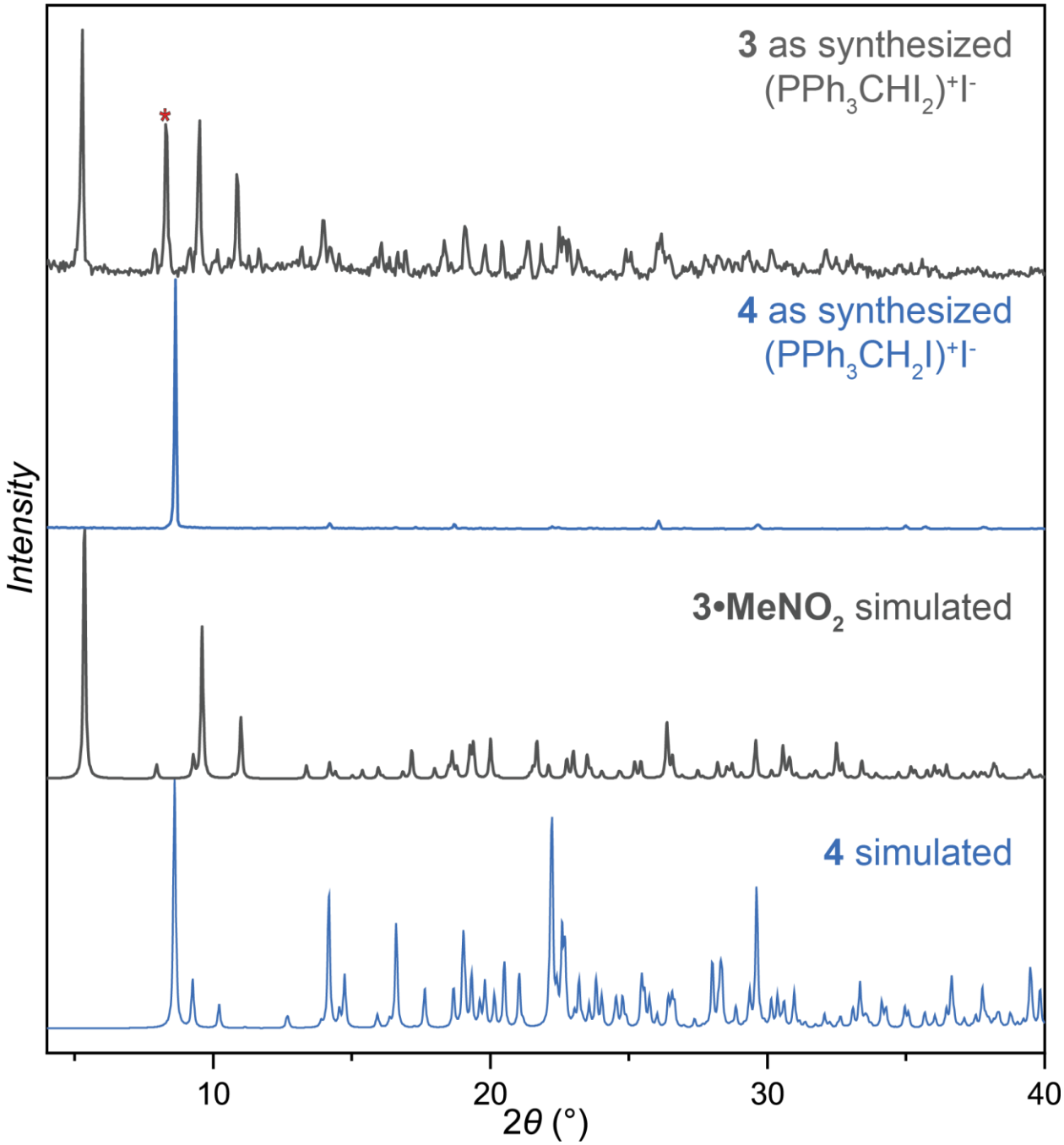

Figure S5.7. Comparison of PXRD patterns of powders of **3** and **4** (from top to bottom): bulk powdered **3** as synthesized from MeCN; bulk powdered **4** as synthesized from hot $MeNO_2$; **3•MeNO** simulated from the scXRD structure reported herein; **4** simulated from the scXRD structure reported herein.

S6. Fourier-transform infrared attenuated total reflectance (FTIR-ATR) spectroscopy

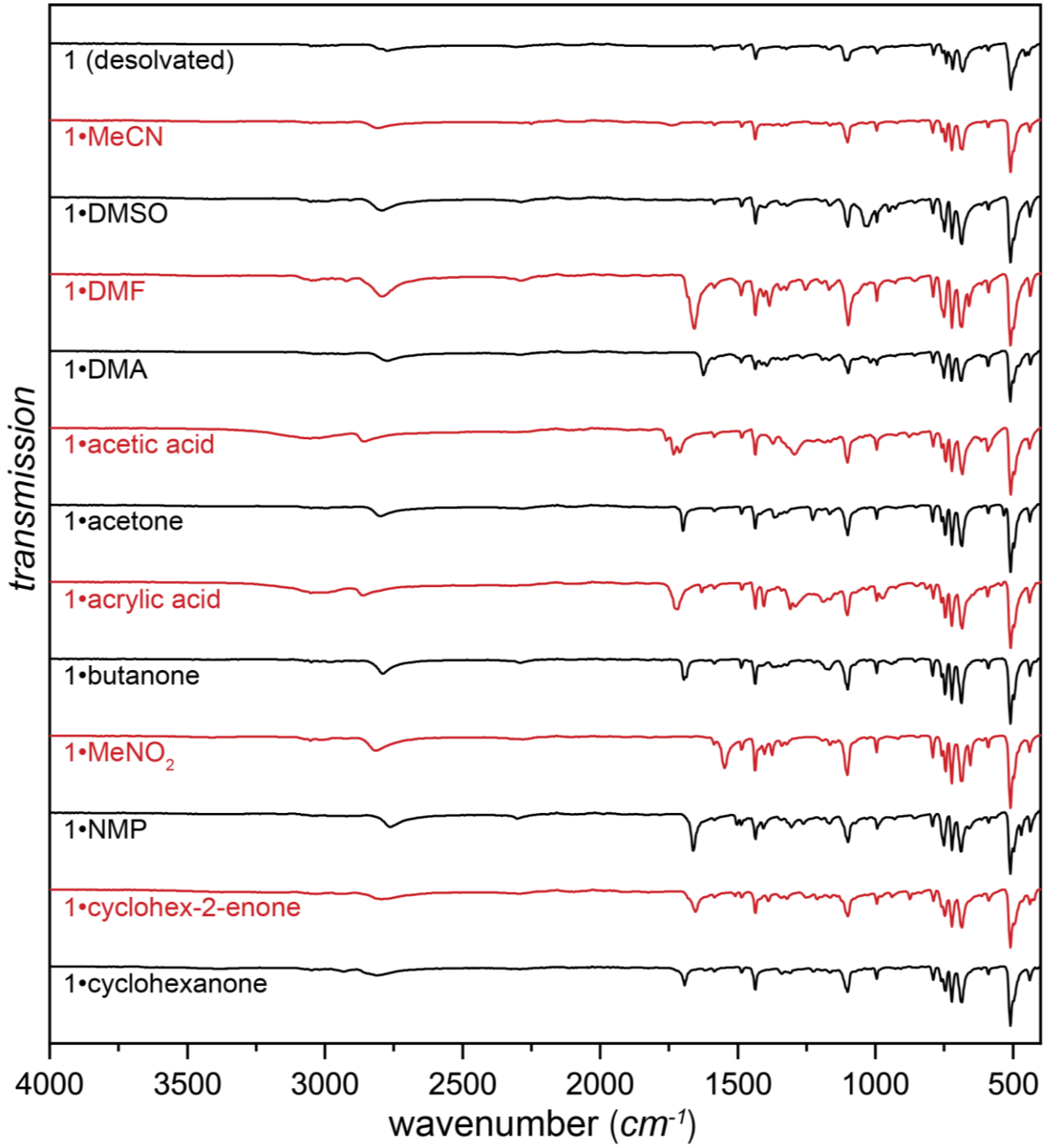

Figure S6.1. Comparison of FTIR-ATR spectra of **1•guest** materials.

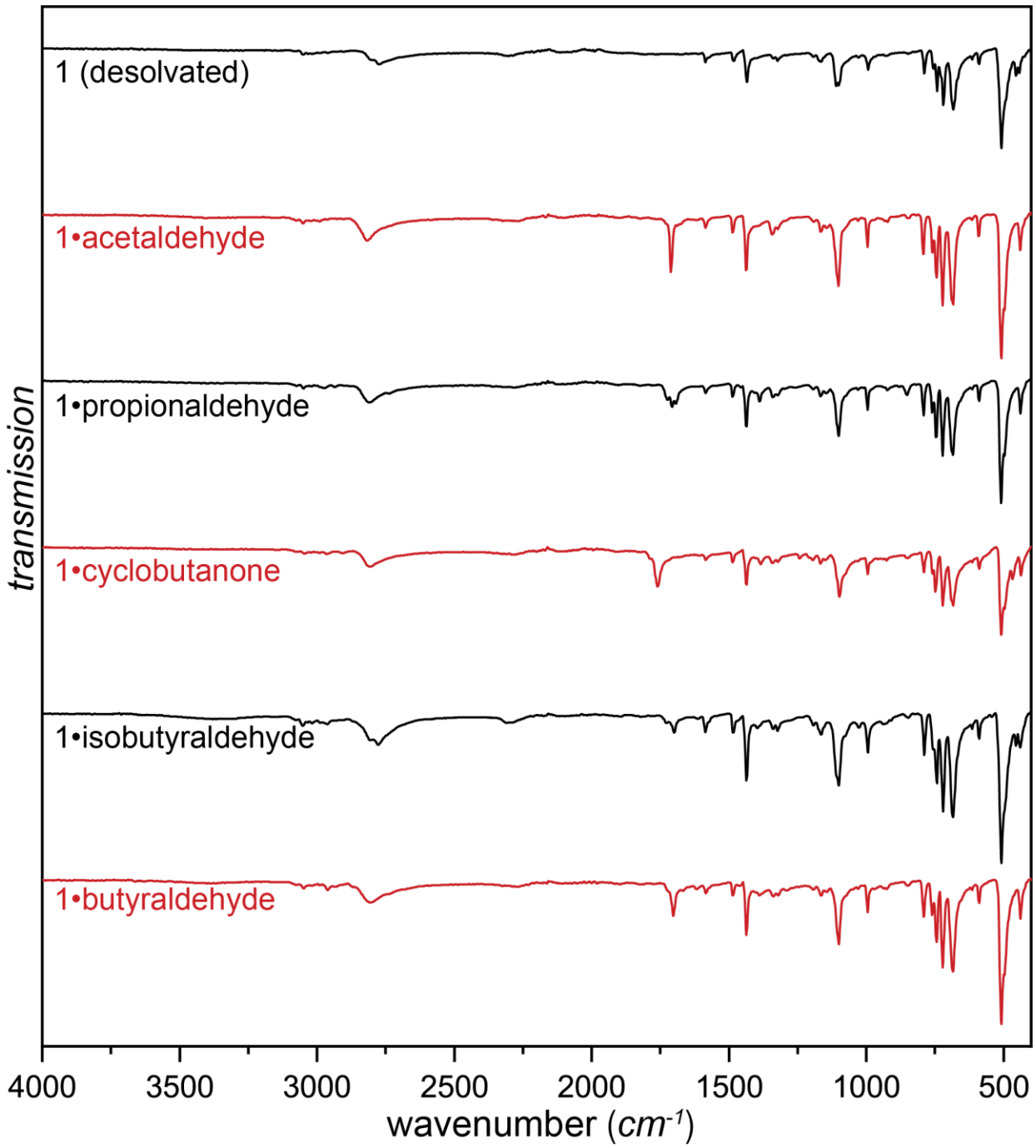

Figure S6.2. Comparison of FTIR-ATR spectra of **1•reactive-guest** materials.

S7. Thermogravimetric analysis

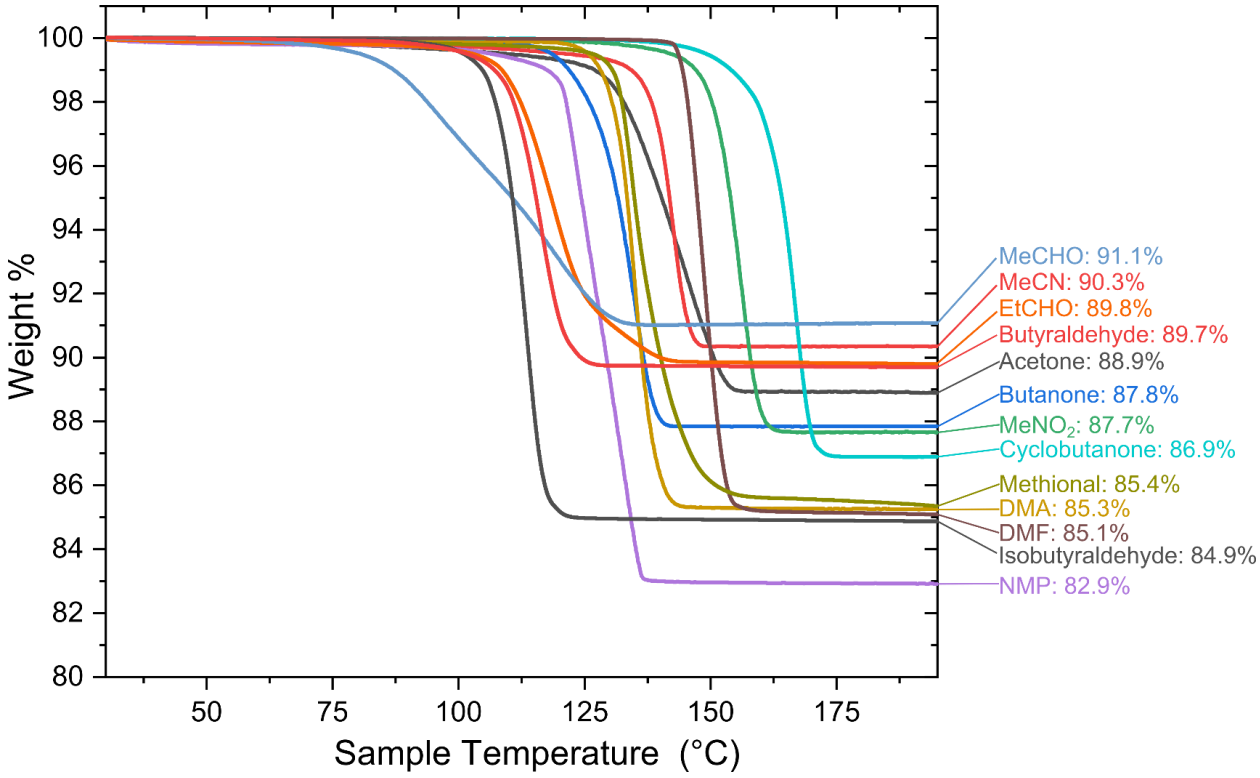

Figure S7.1. TGA thermograms **1•guest** and **1•reactive-guest** materials for which the regions before and after the initial loss of mass were sufficiently flat to allow for the calculation of guest quantities.

Number of guests per cage was calculated from TGA residues using the following equation:

$$Residue\ \% = \frac{6M_r(\mathbf{1})}{6M_r(\mathbf{1}) + nM_r(\boldsymbol{guest})} * 100$$

where:

n = number of guests per hexameric cage

$M_r(\mathbf{1})$ = molecular weight of **1**

$nM_r(\boldsymbol{guest})$ = molecular weight of the **guest**

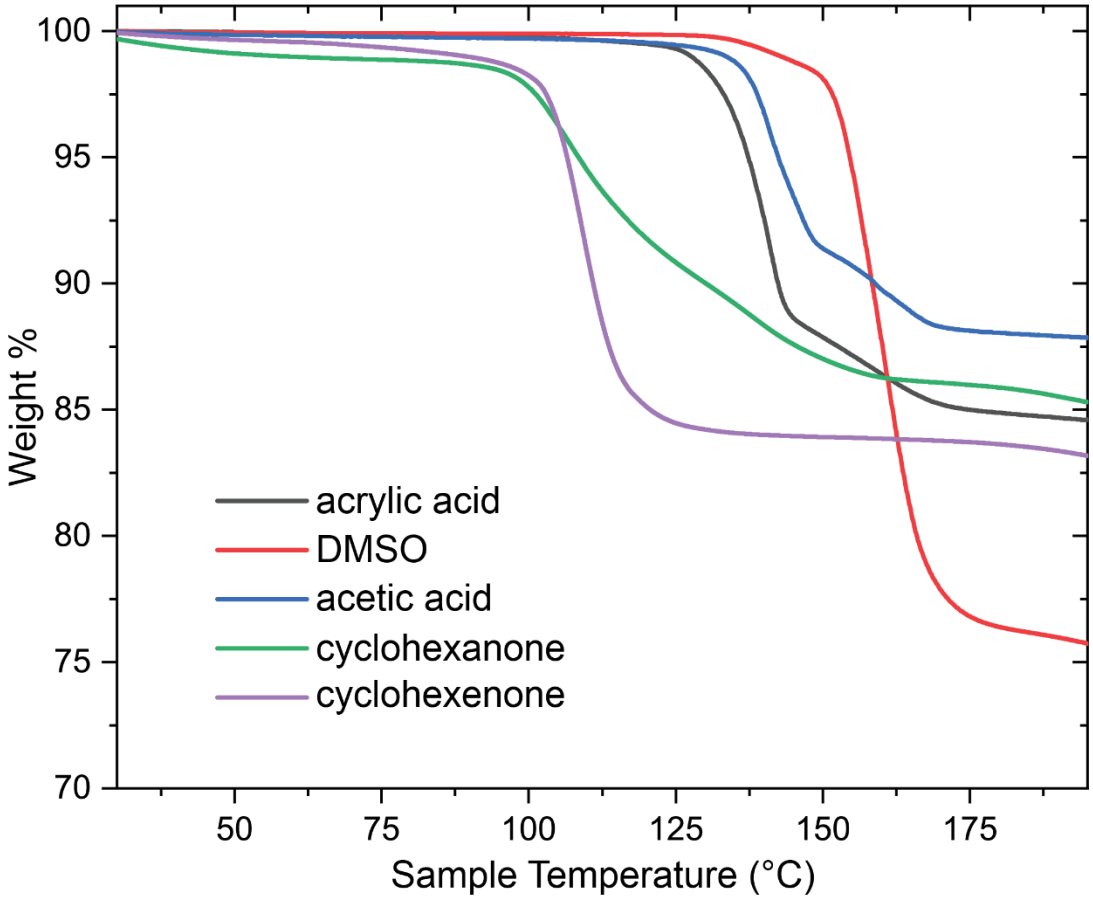

Figure S7.2. TGA thermograms **1•guest** and **1•reactive-guest** materials for which the regions before or after the initial loss of mass were not sufficiently flat to allow for the calculation of guest quantities.

S8. Number of guest molecules per cage in 1·guest materials as determined by TGA and NMR

Table S8.1. The number of guests per cage in **1·guest** materials as determined by TGA and ^{1}H NMR. The corresponding TGA data and the method for the calculation of guest loading based on it are shown in section **S7.** Calculations based on ^{1}H NMR are explained in section **S10.1.** and the raw data is shown in section **S11**.

material	guests per cage (TGA)	guests per cage (^{1}H NMR)
1•acetaldehyde	6.9	6.5
1•MeCN	8.1	6.8
1•propionaldehyde	6.0	5.9
1•acetone	6.6	5.7
1•butanone	6.0	5.6
1•$MeNO_2$	7.1	6.2
1•cyclobutanone	6.7	6.2
1•methional	5.1	3.6
1•DMA	6.1	6.0
1•DMF	7.4	6.8
1•NMP	6.4	6.0
1•isobutyraldehyde	7.7	4.3
1•butyraldehyde	4.9	4.4
1•acetic acid	-	7.1
1•acrylic acid	-	-*
1•DMSO	-	7.0
1•cyclohex-2-enone	-	5.4
1•cyclohexanone	-	4.4

*: The ^{1}H NMR for 1•**acrylic acid** contains impurities which obscure signals from acrylic acid, making determination of guests per cage impossible.

S9. Analysis of Organic Products

Raw ^{1}H and ^{13}C spectra are presented in section **S13.**

1,1-dibromopropene

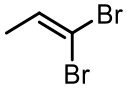

Colorless liquid isolated by distillation from the contents of the jar after milling. ^{1}H NMR (500 MHz, $CDCl_3$): 1.71 (d, J = 6.8 Hz, 3H), 6.46 (q, J = 6.8 Hz, 1H). ^{13}C NMR (125 MHz, $CDCl_3$): 18.5 (CH_3), 89.6 ($C_{dibromo}$), 133.5 (CH). GCMS (m/z): [M]+ calculated for $C_3H_4Br_2$: 199.9; found: 200.

1,1-dibromobutene

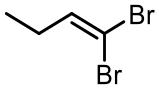

Colorless liquid, isolated by distillation from jar contents. ^{1}H NMR (500 MHz, $CDCl_3$): 1.04 (t, J = 7.5 Hz, 3H), 2.12 (p, J = 7.5 Hz, 2H), 6.40 (t, J = 7.2 Hz, 1H). ^{13}C NMR (125 MHz, $CDCl_3$): 12.3 (CH_3), 26.5 (CH_2), 88.2 ($C_{dibromo}$), 140.1 (CH). GCMS (m/z): [M]+ calculated for $C_3H_4Br_2$: 213.9; found: 214.

1,1-dibromopentene

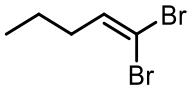

Colorless liquid, isolated by distillation from jar contents. ^{1}H NMR (500 MHz, $CDCl_3$): 0.95 (t, J = 7.4 Hz, 3H), 1.46 (h, J = 7.4 Hz, 2H), 2.09 (q, J = 7.3 Hz, 2H), 6.41 (t, J = 7.2 Hz, 1H). ^{13}C NMR (125 MHz, $CDCl_3$): 13.6 (CH_3), 21.2 (CH_2), 35.0 (CH_2), 88.6 ($C_{dibromo}$), 138.7 (CH). GCMS (m/z): [M]+ calculated for $C_5H_8Br_2$: 227.9; found: 228.

(dibromomethylene)cyclobutane

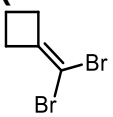

Colorless liquid, isolated by column chromatography in 100% hexanes. ^{1}H NMR (500 MHz, $CDCl_3$): 1.91 (p, J = 8.0 Hz, 2H), 2.63 (t, J = 8.0 Hz, 2H). ^{13}C NMR (125 MHz, $CDCl_3$): 13.4 (CH_2), 32.6 (CH_2), 78.9 ($C_{dibromo}$), 147.3 (C). GCMS (m/z): [M]+ calculated for $C_5H_8Br_2$: 225.9; found: 226.

1,1-dibromo-4-methylthiobutene

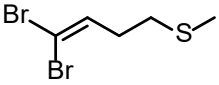

Colorless liquid, isolated by column chromatography in 100% hexanes. ^{1}H NMR (500 MHz, $CDCl_3$): 2.14 (s, 3H), 2.41 (q, J = 7.2 Hz, 2H), 2.59 (t, J = 7.3 Hz, 2H), 6.50 (t, J = 7.1 Hz, 1H). ^{13}C NMR (125 MHz, $CDCl_3$): 15.4 (CH_3), 32.0 (CH_2), 32.5 (CH_2), 90.3

($C_{dibromo}$), 136.5 (CH). APCI-HRMS (m/z): [M+H]+ calculated for $C_5H_9Br_2S$: 258.88 ; found: 258.88.

eneyne Sonogashira product

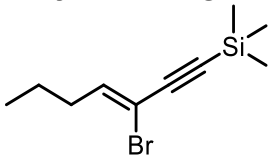

Yellow oil, isolated by column chromatography in 100% hexanes. Co-elutes with trimethylsilylacetylene homocoupling dimer, marked in NMR spectra. ^{1}H NMR (500 MHz, $CDCl_3$): 0.22 (s, 9H), 0.96 (t, J = 7.4 Hz, 3H), 1.47 (h, J = 7.3 Hz, 2H), 2.21 (q, J = 7.3 Hz, 2H), 6.35` (t, J = 7.2 Hz, 1H). ^{13}C NMR (125 MHz, $CDCl_3$): -0.3 ($CH_{3\ TMS}$), 13.7 (CH_3), 21.2 (CH_2), 34.0 (CH_2), 94.6 (C), 102.6 (C), 102.6 (C), 141.1 (CH). APCI-HRMS (m/z): [M]+ calculated for $C_{10}H_{17}BrSi$: 244.03; found: 244.03.

enediyne Sonogashira product

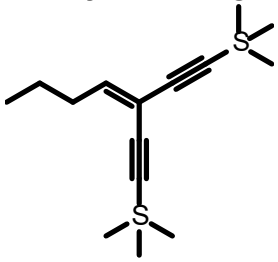

Yellow oil, isolated by column chromatography in 100% hexanes. ^{1}H NMR (500 MHz, $CDCl_3$): 0.20 (s, 9H), 0.22 (s, 9H), 0.95 (t, J = 7.4 Hz, 3H), 1.47 (h, J = 7.4 Hz, 2H), 2.33 (q, J = 7.4 Hz, 2H), 6.42 (t, J = 7.7 Hz, 1H). ^{13}C NMR (125 MHz, $CDCl_3$): -0.1 ($CH_{3\ TMS}$), 13.8 (CH_3), 21.7 (CH_2), 32.8 (CH_2), 91.5 (C), 98.4 (C), 99.8 (C), 102.5 (C), 106.0 (C), 151.8 (CH). APCI-HRMS (m/z): [M]+ calculated for $C_{15}H_{26}Si_2$: 262.16; found: 262.16.

enediyne Sonogashira product (thioether analogue)

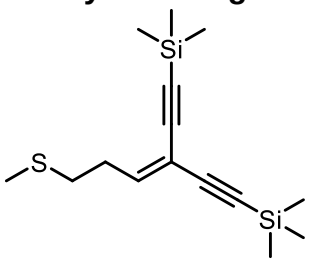

Yellow oil, isolated by column chromatography using a gradient elution from 100% hexanes to 5% ether in hexanes. ^{1}H NMR (500 MHz, $CDCl_3$): 0.20 (s, 9H), 0.22 (s, 9H), 0.95 (t, J = 7.4 Hz, 3H), 1.47 (h, J = 7.4 Hz, 2H), 2.33 (q, J = 7.4 Hz, 2H), 6.42 (t, J = 7.7 Hz, 1H). ^{13}C NMR (125 MHz, $CDCl_3$): -0.18 ($CH_{3\ TMS}$) -0.15 ($CH_{3\ TMS}$), 15.3 (CH_3), 30.3 (CH_2), 32.5 (CH_2), 92.4 (C), 99.1 (C), 99.4 (C), 102.0 (C), 107.2 (C), 148.5 (CH). APCI-HRMS (m/z): [M+H]+ calculated for $C_{15}H_{27}SSi_2$: 295.13; found: 295.13.

S10. ^{1}H NMR quantitative methods

S10.1. Calculation of the number of guests per cage

The phenyl group protons of **1** are used as an internal standard. Integrations are such that the signals which correspond to six protons of **1** are set to an integration value of 1.0. A characteristic signal of the **guest** molecule is chosen, its integration divided by the number of protons it corresponds to per each **guest** molecule, then multiplied by six to obtain the number of guests per salt **1**. Multiplying this number by 6 gives the approximate number of guest molecules per hexameric cage.

S10.2. Calculation of conversion for Wittig Olefination reactions

Conversions of Wittig olefination reactions were determined by comparing integrations of characteristic signals from the 1,1-dihaloolefin product with characteristic signals from the aldehyde or ketone guest.

S10.3. Calculation of conversion for one-pot combination of Wittig Olefination and Sonogashira coupling reactions

Originally, a method identical the one for the calculation of yields for the Wittig olefinations (**S10.2.**) was used for the one-pot reactions, where the ^{1}H NMR signal integrations for starting materials and olefin products were directly compared. However, conversions determined in this way showed a marked discrepancy from isolated yields, so an alternative method was used which matches yields and conversions more accurately.

In this method, the reaction byproduct triphenylphosphine oxide (TPPO) was used as an internal standard. This method assumes that one equivalent of cage material produces one equivalent of TPPO during the reaction. Given the known initial quantity of cage material and guest, all product signal integrations can be compared to TPPO, to derive an approximate conversion. Importantly, this method accounts for reactant or product which may be lost to processes like polymerization or decomposition, so the calculated conversions are uniformly lower, but more realistic, than they are for the original method.

S11. ^{1}H NMR of cage materials

In spectra of **1•guest** materials, the characteristic ^{1}H NMR signal for the guest which is integrated and compared to signals of the guest is denoted by a red "*" (asterisk).

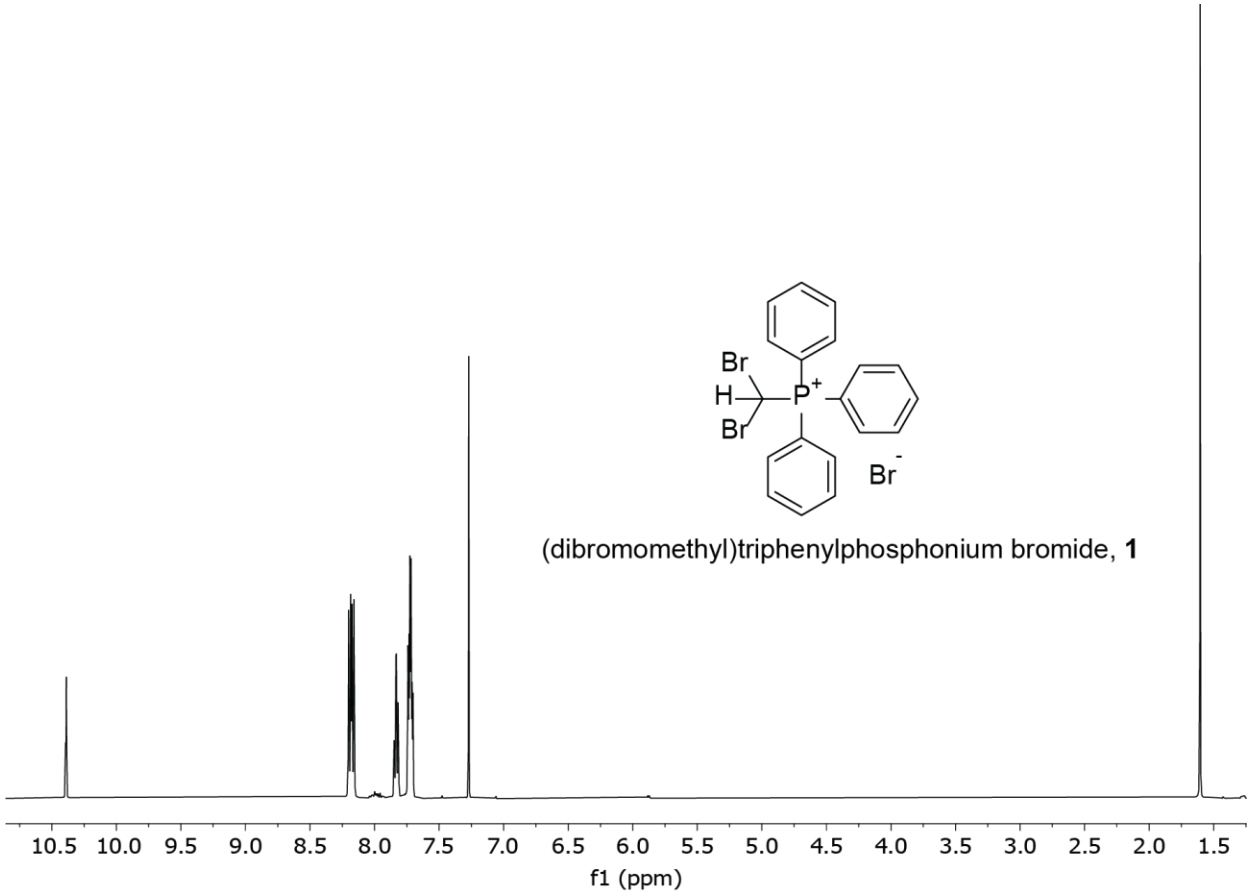

Figure S11.1. ^{1}H NMR of pure desolvated **1**

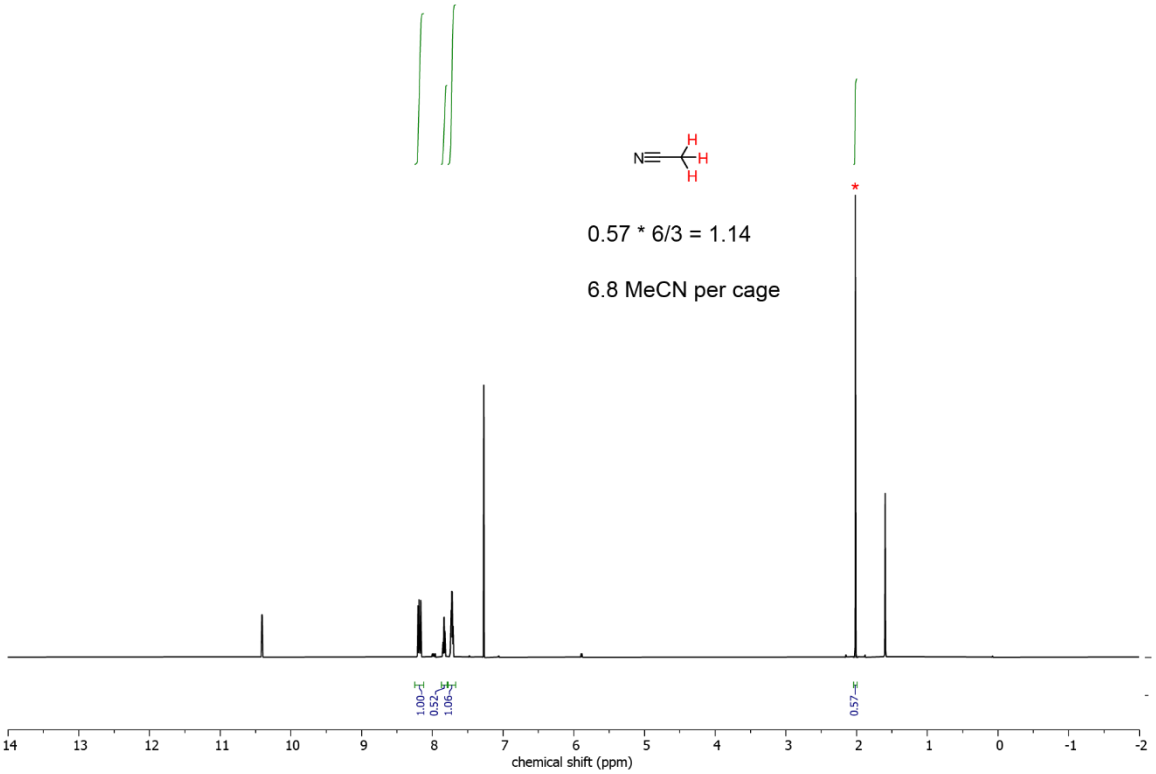

Figure S11.2. ^{1}H NMR of **1•MeCN**

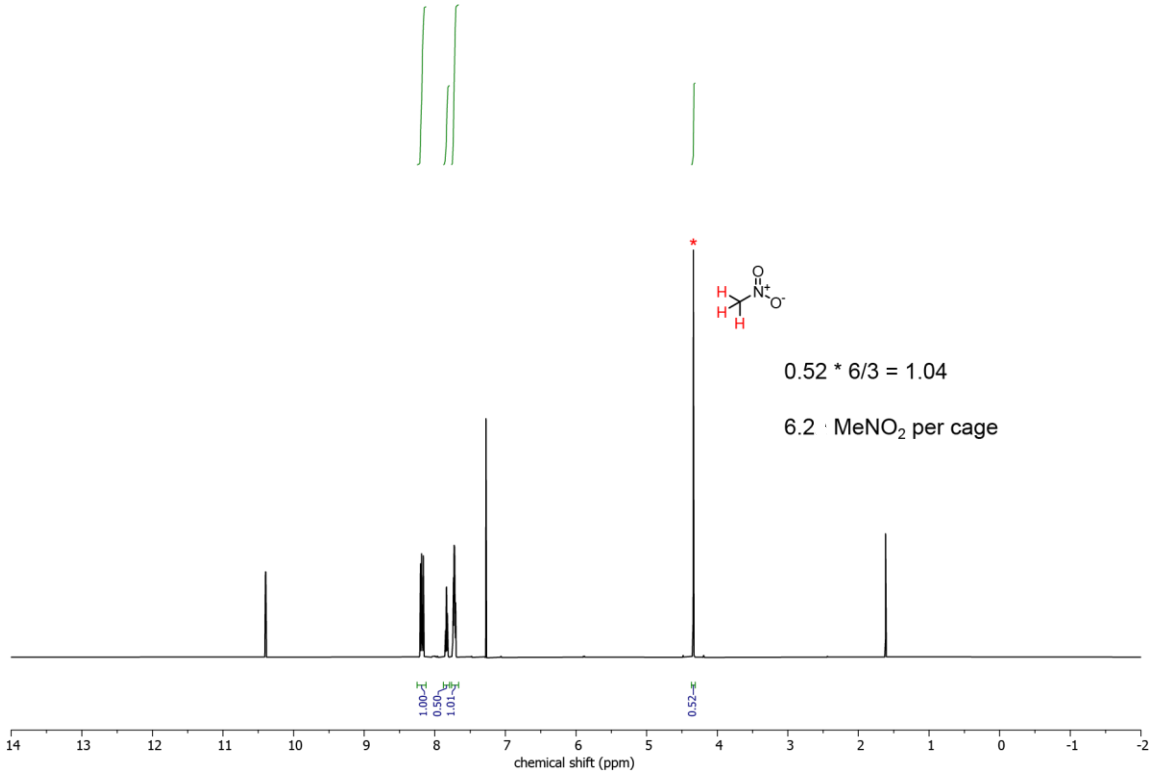

Figure S11.3. ^{1}H NMR of **1•MeNO$_2$**

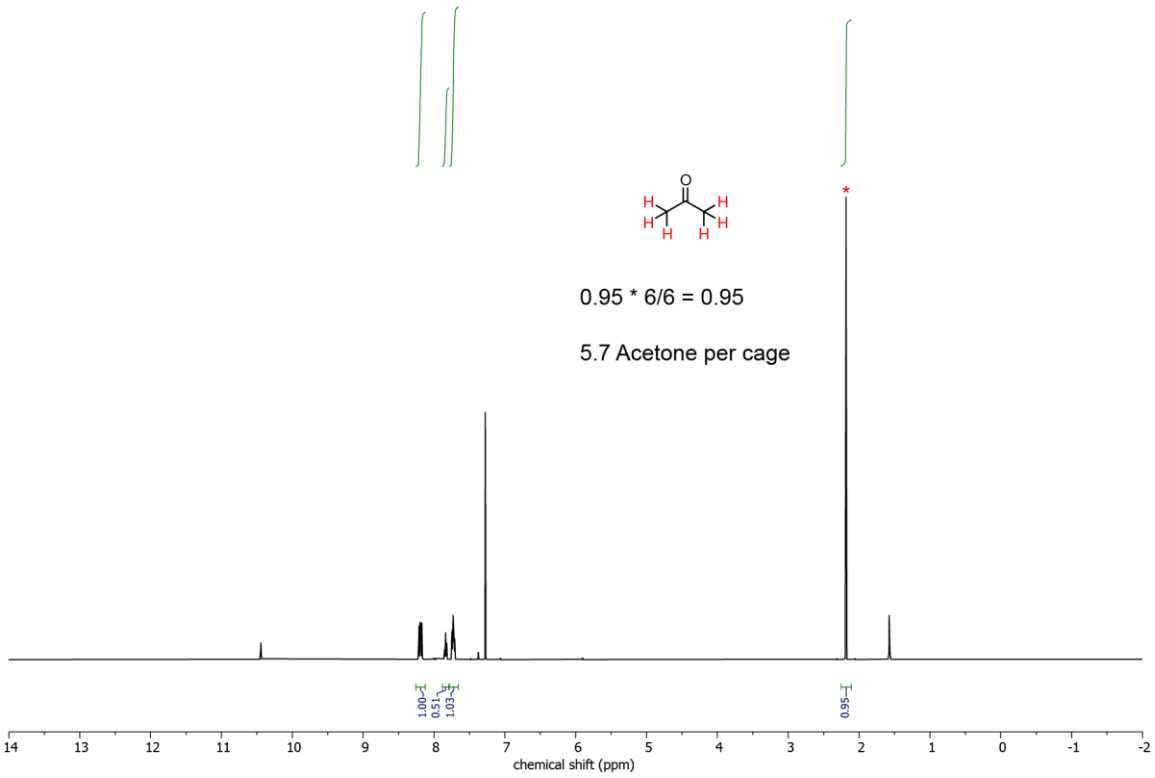

Figure S11.4. ^{1}H NMR of **1•acetone**

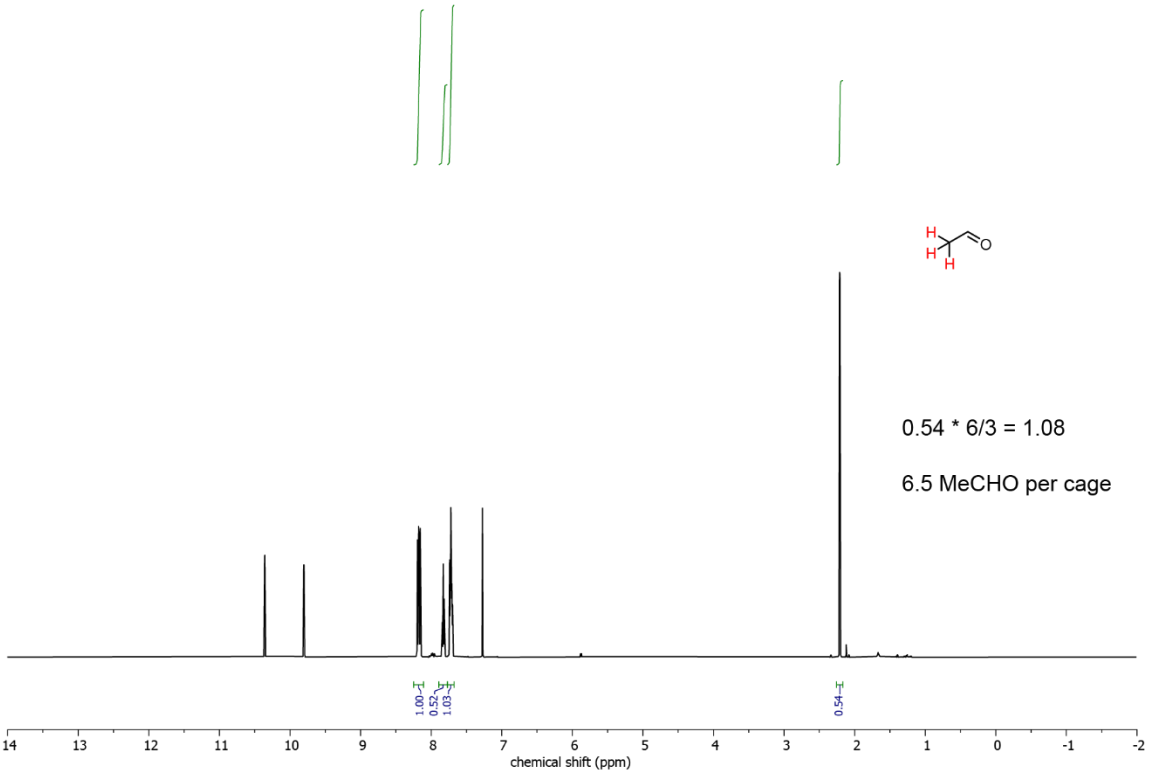

Figure S11.5. ^{1}H NMR of **1•acetaldehyde**

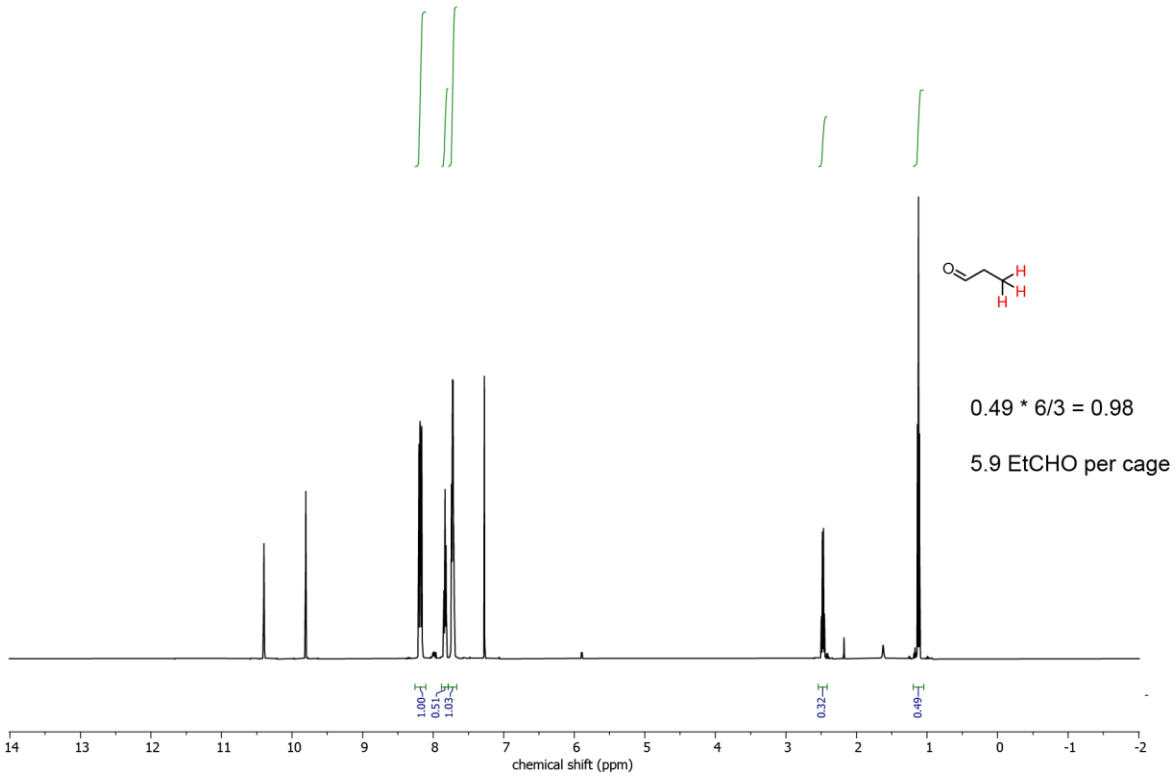

Figure S11.6. ^{1}H NMR of **1•propionaldehyde**

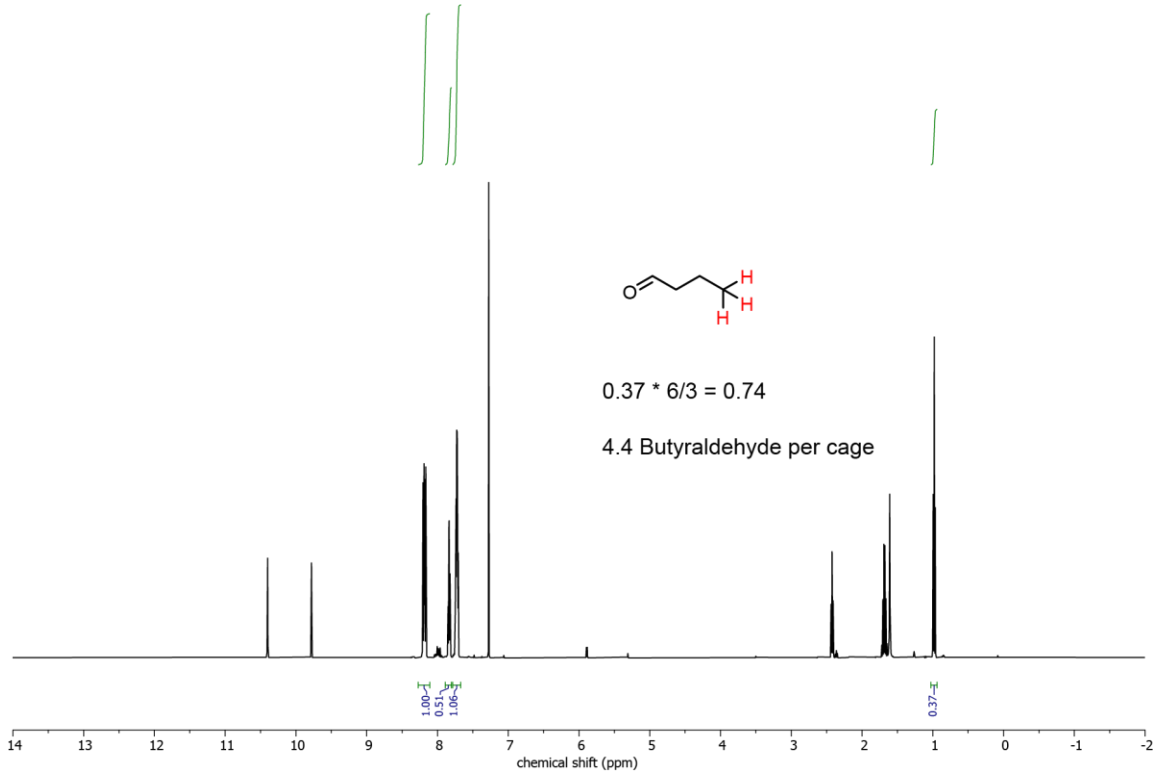

Figure S11.7. ^{1}H NMR of **1•butyraldehyde**

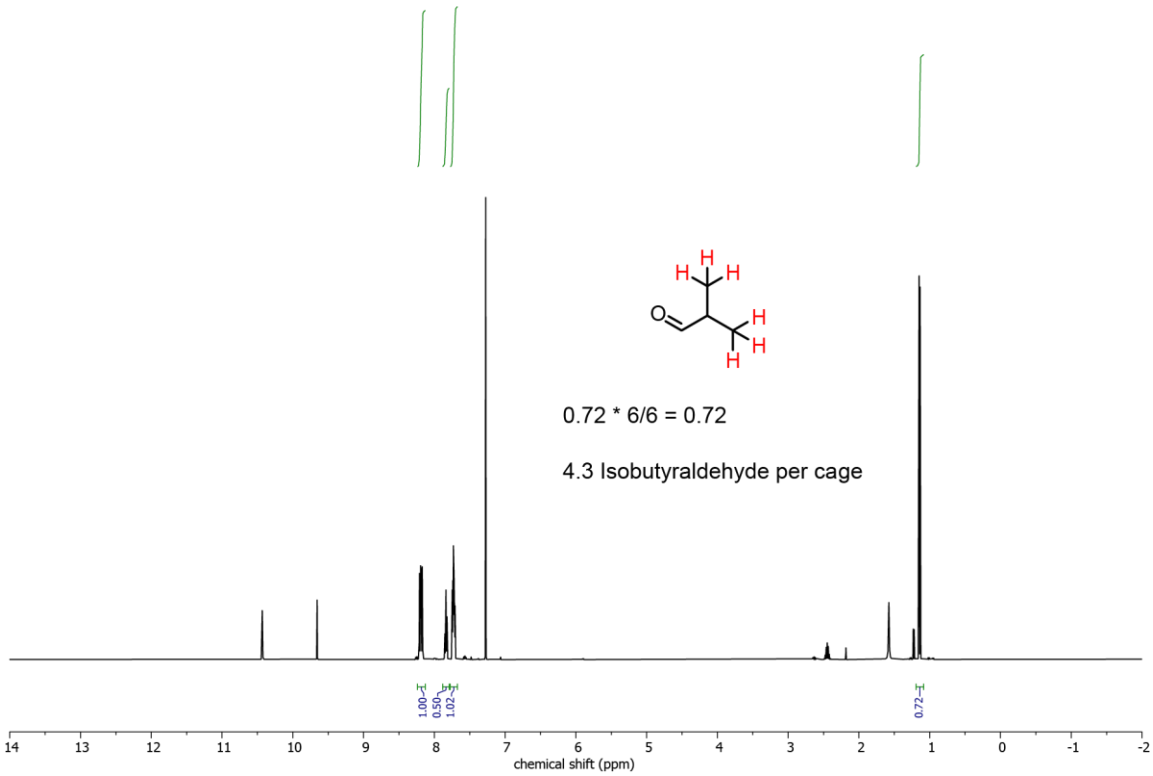

Figure S11.8. ^{1}H NMR of **1•isobutyraldehyde**

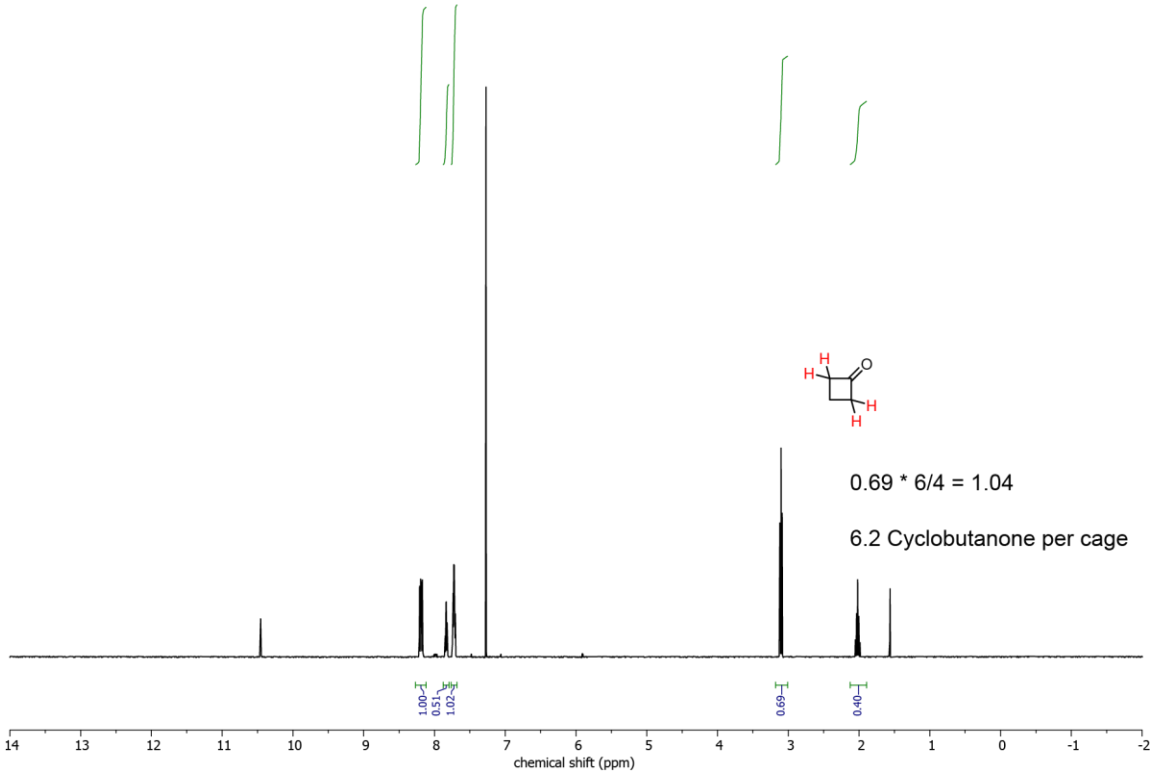

Figure S11.9. ^{1}H NMR of **1•cyclobutanone**

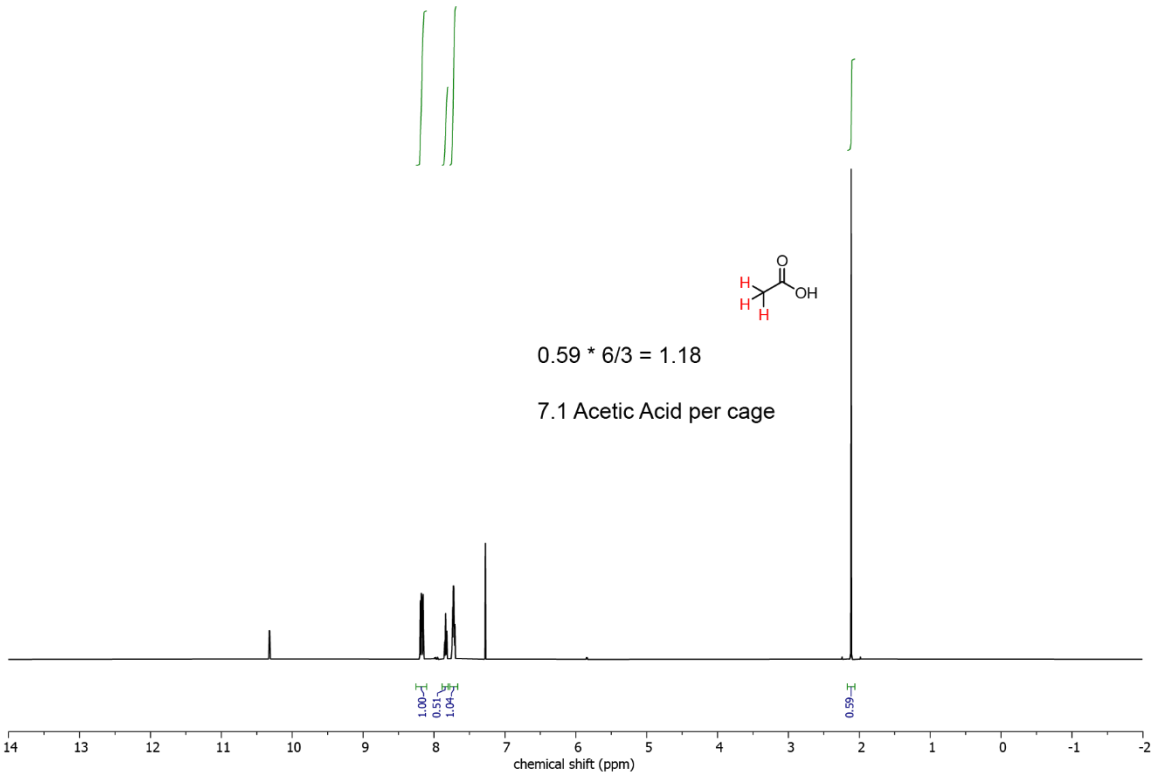

Figure S11.10. ^{1}H NMR of **1•acetic acid**

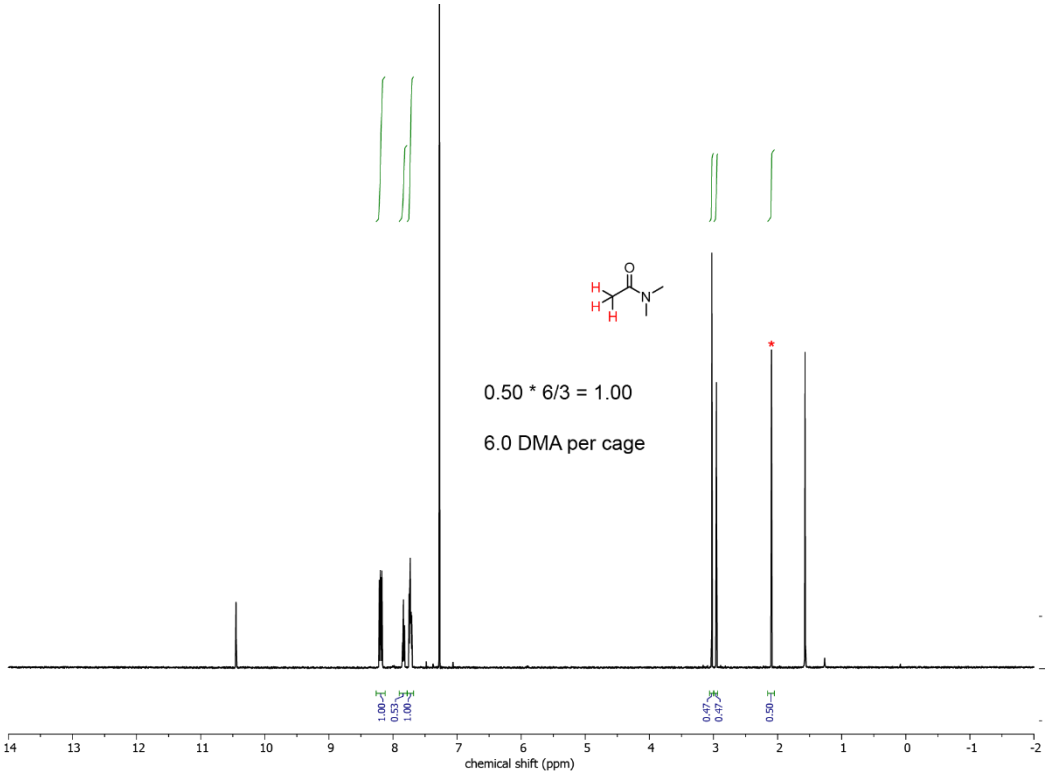

Figure S11.11. ^{1}H NMR of **1•DMA**

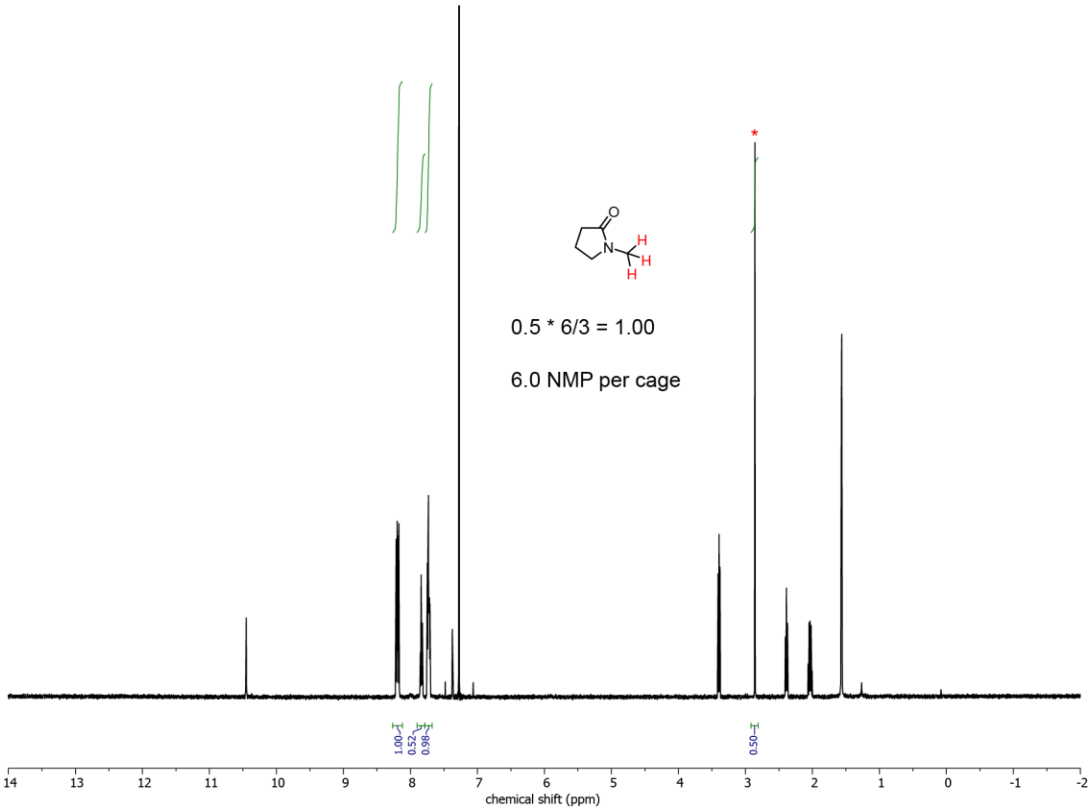

Figure S11.12. ^{1}H NMR of **1•NMP**

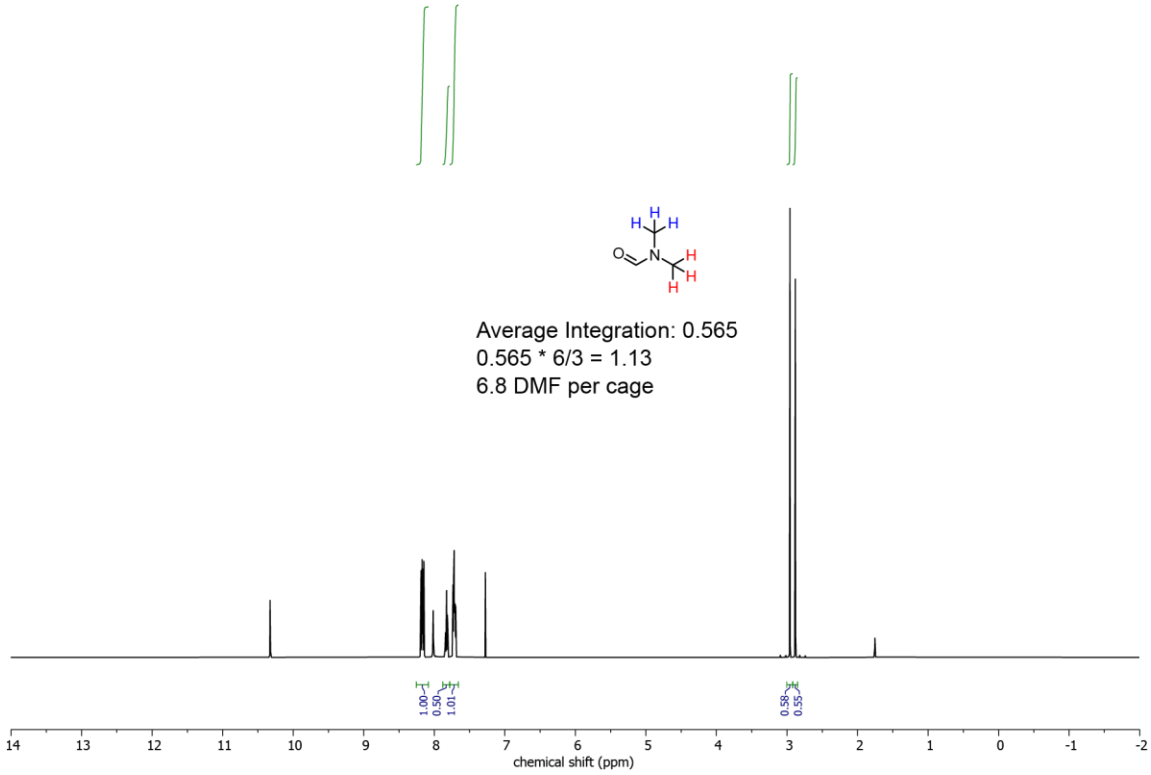

Figure S11.13. ^{1}H NMR of **1•DMF**

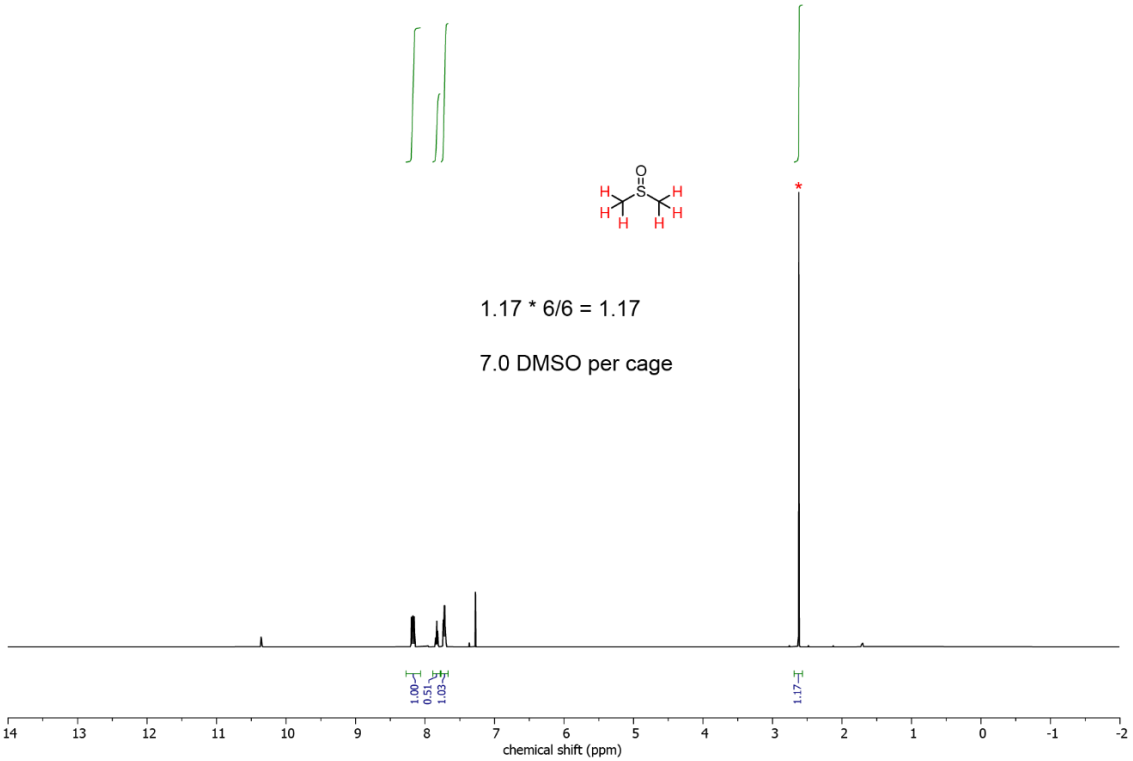

Figure S11.14. ^{1}H NMR of **1•DMSO**

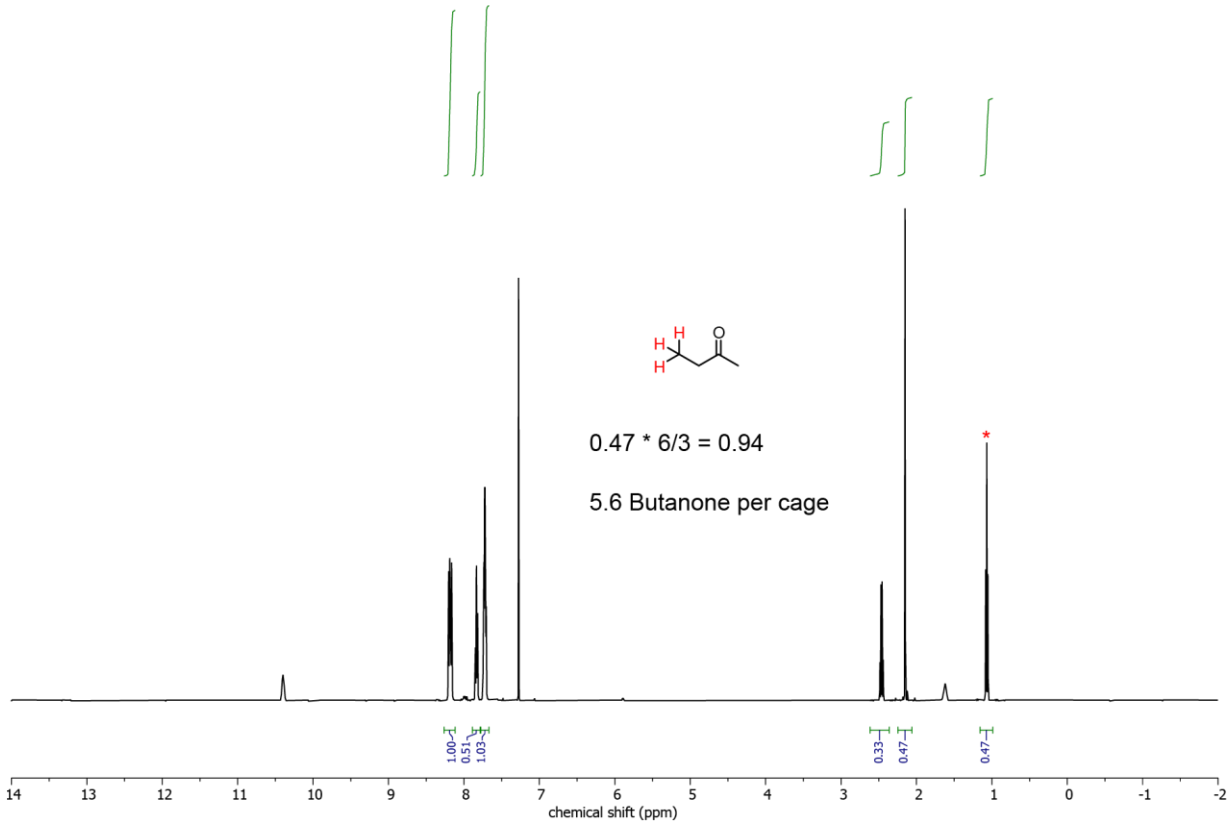

Figure S11.15. ^{1}H NMR of **1•butanone**

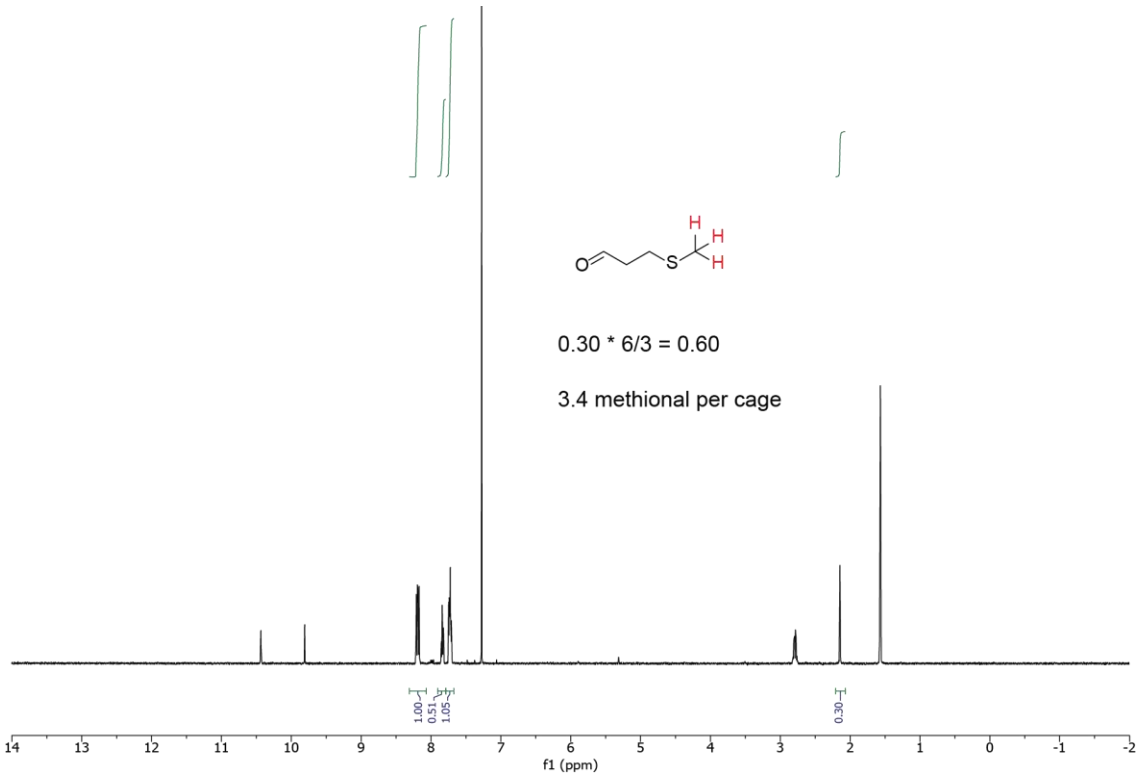

Figure S11.16. ^{1}H NMR of **1•methional**

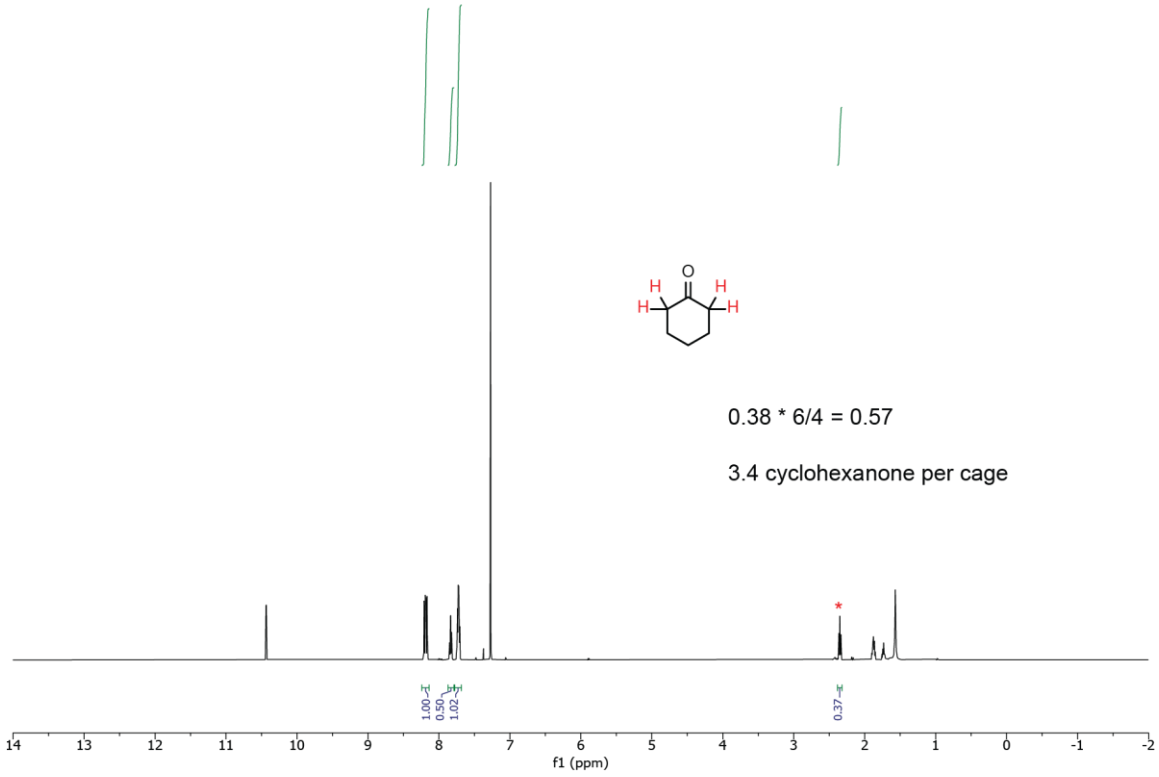

Figure S11.17. ^{1}H NMR of **1•cyclohexanone**

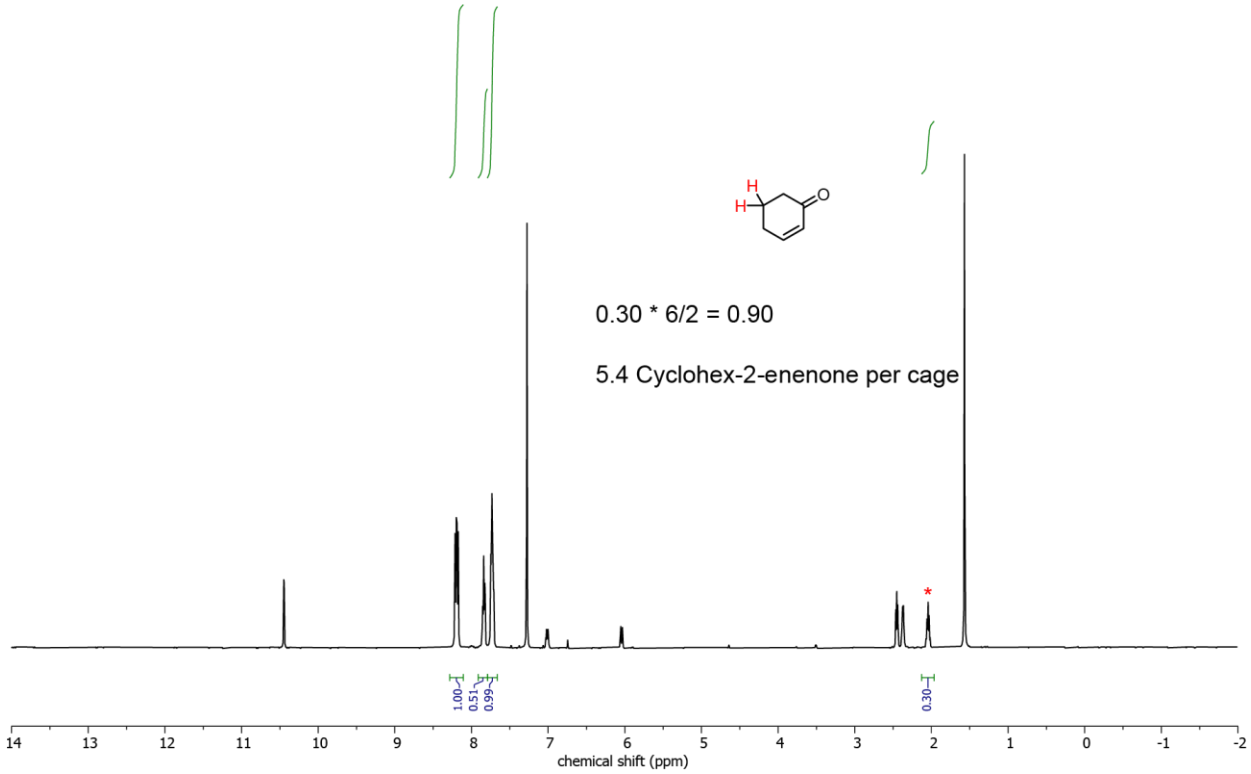

Figure S11.18. ^{1}H NMR of **1•cyclohex-2-enenone**

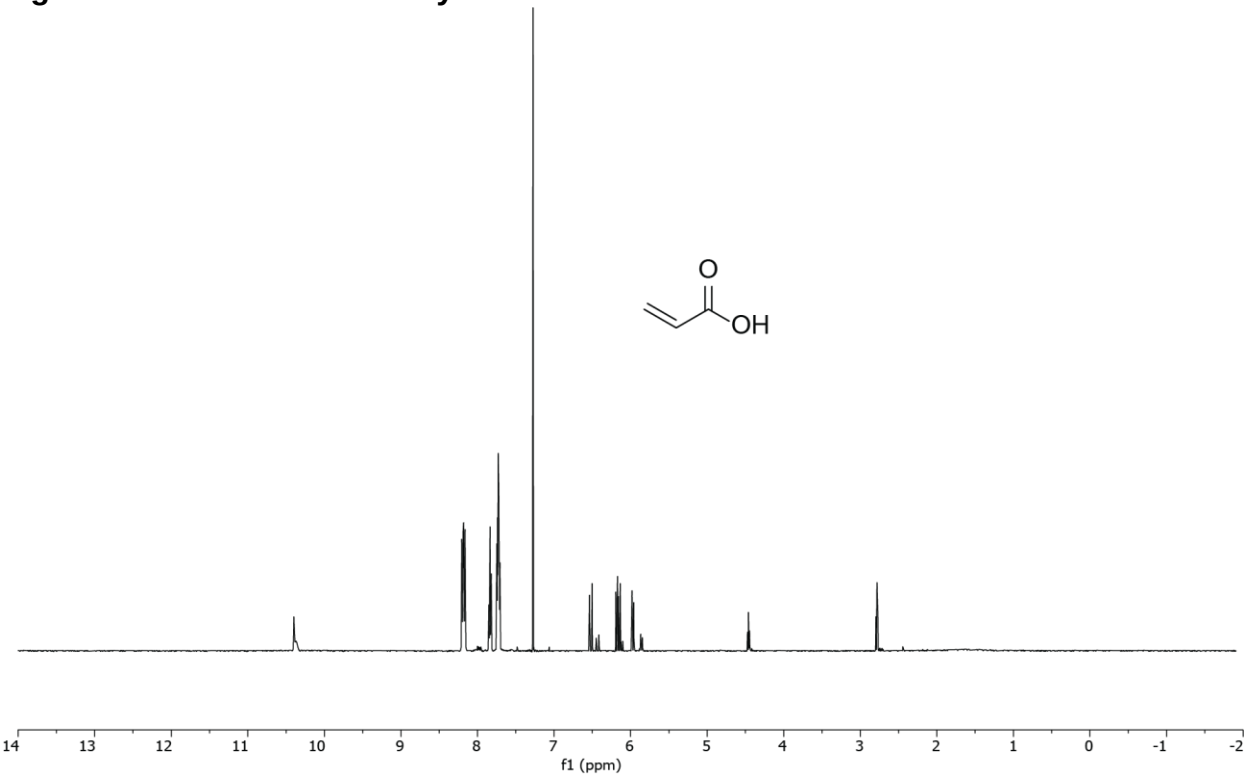

Figure S11.19. ^{1}H NMR of **1•acrylic acid**

S12. ^{1}H NMR of crude milling products after Wittig olefination

In each spectra, relative intensities for each relevant peak are labeled “I”. These values are compared to determine conversions as discussed in **S10.2.**

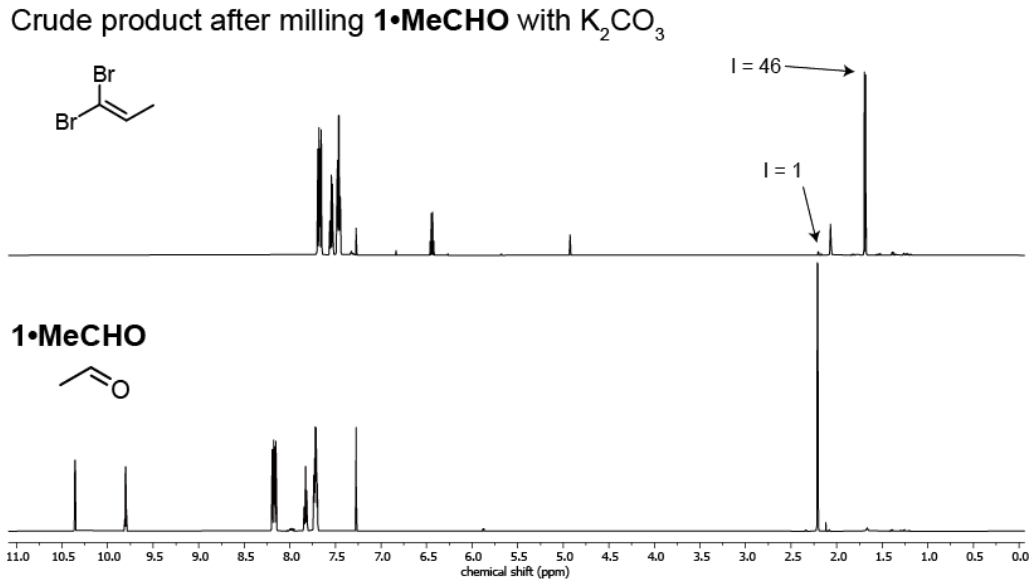

Figure S12.1. ^{1}H NMR spectra of **1•MeCHO** and the crude product of milling **1•MeCHO** with a base.

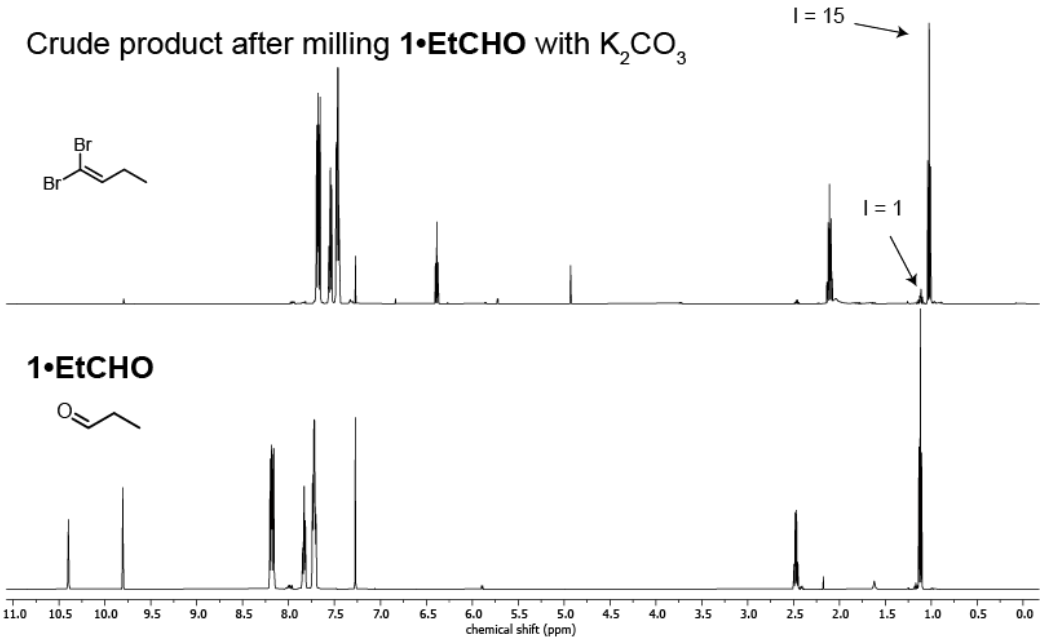

Figure S12.2. ^{1}H NMR spectra of **1•EtCHO** and the crude product of milling **1•EtCHO** with a base.

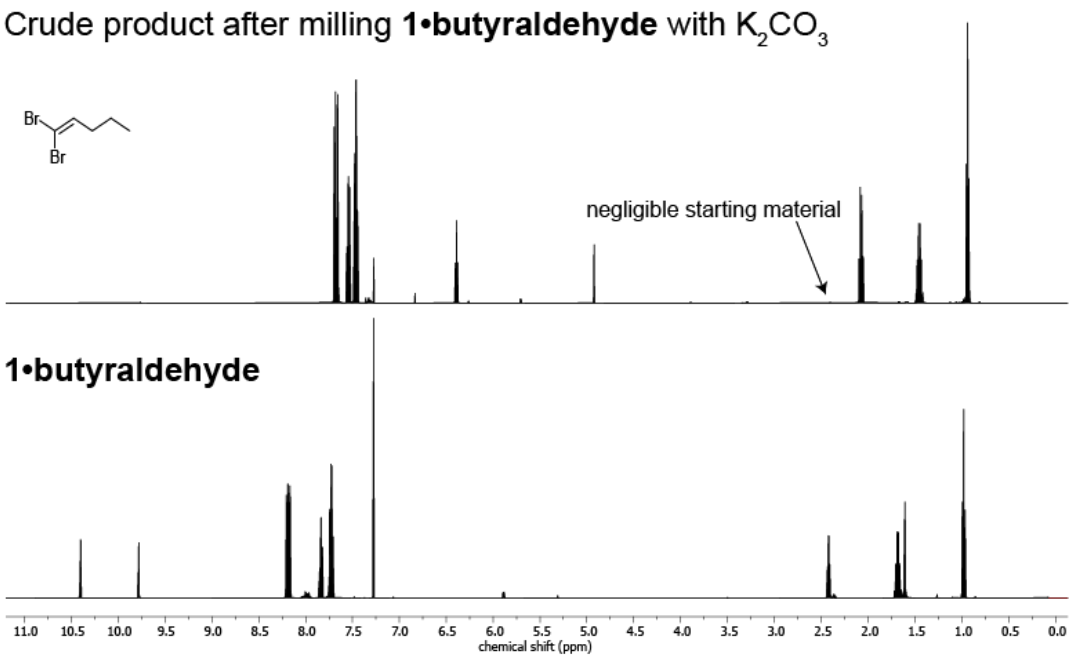

Figure S12.3. ^{1}H NMR spectra of **1•butyraldehyde** and the crude product of milling **1•butyraldehyde** with a base.

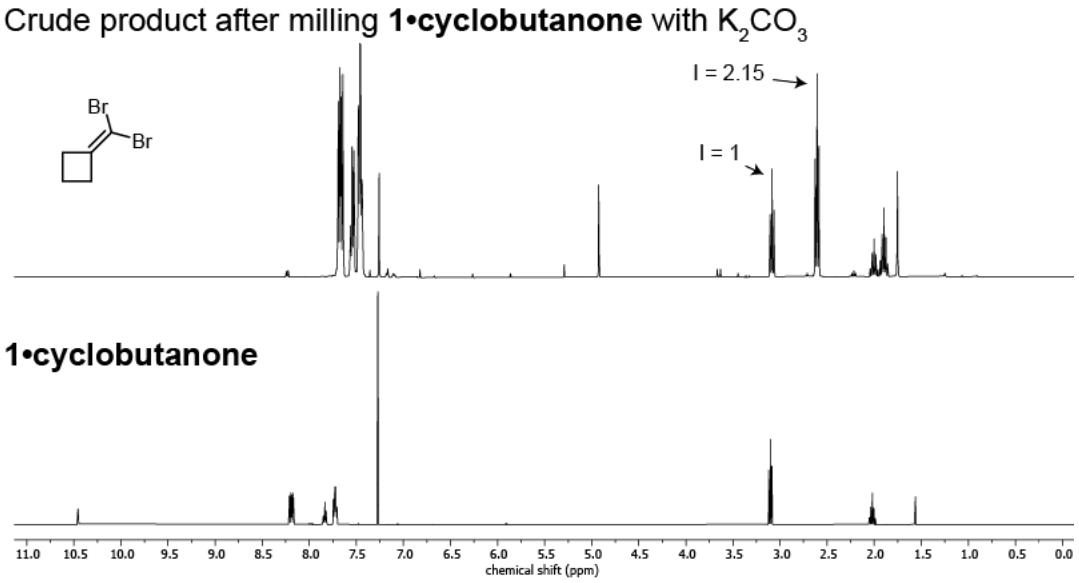

Figure S12.4. ^{1}H NMR spectra of **1•cyclobutanone** and the crude product of milling **1•cyclobutanone** with a base.

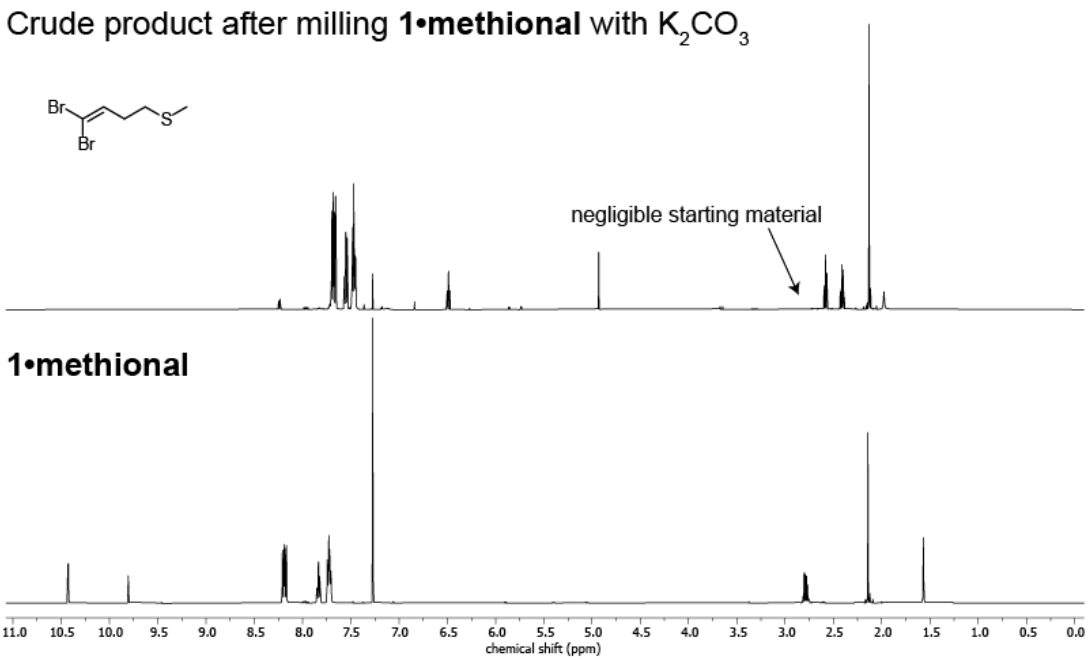

Figure S12.5. ^{1}H NMR spectra of **1•methional** and the crude product of milling **1•methional** with a base.

S13. ^{1}H and ^{13}C NMR spectra of purified products

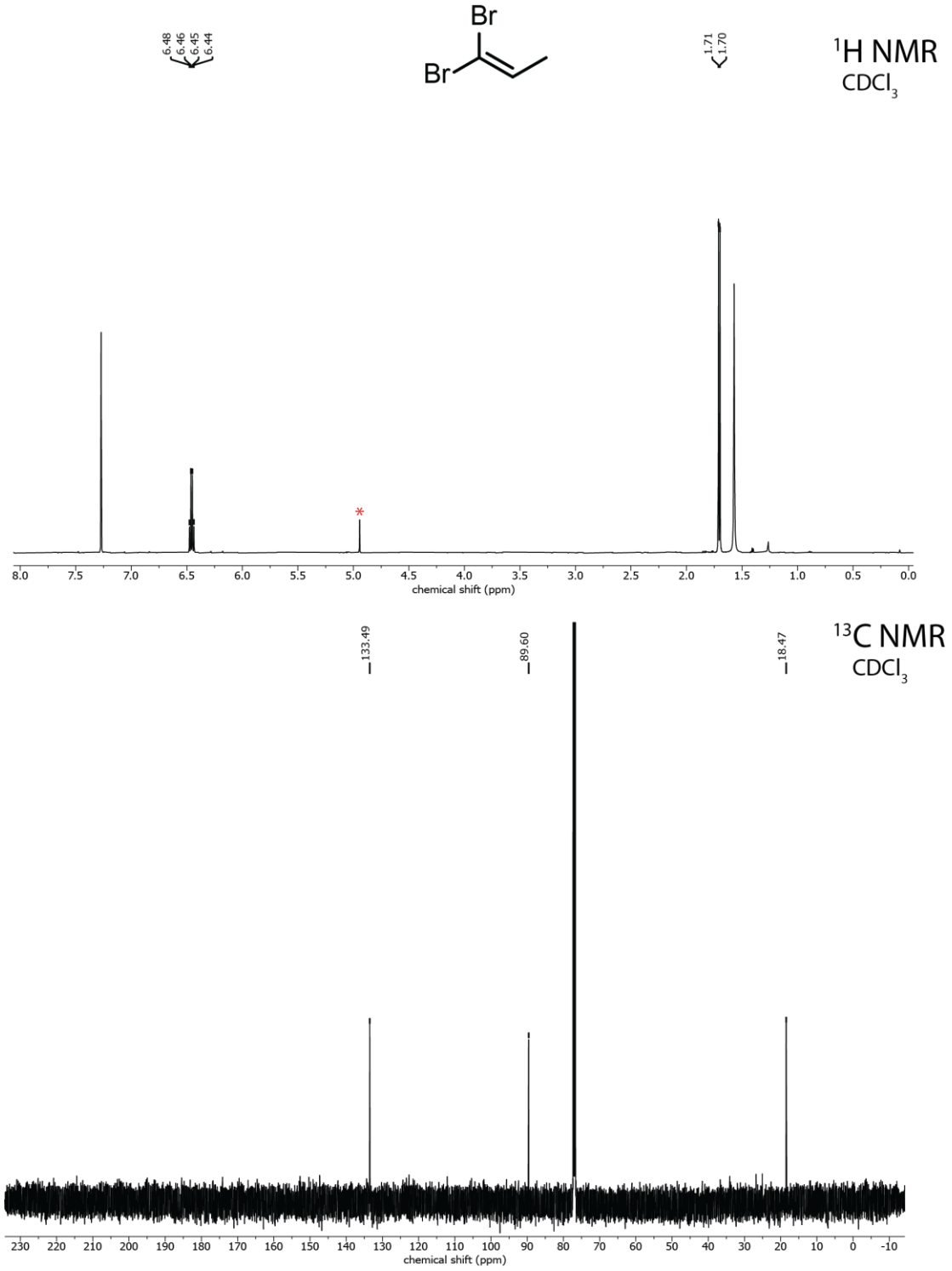

Figure S13.1. ^{1}H and ^{13}C NMR spectra of purified 1,1-dibromopropene produced by mechanochemical Wittig olefination using **1•acetaldehyde**. Signals of the dibromomethane impurity marked with "*".

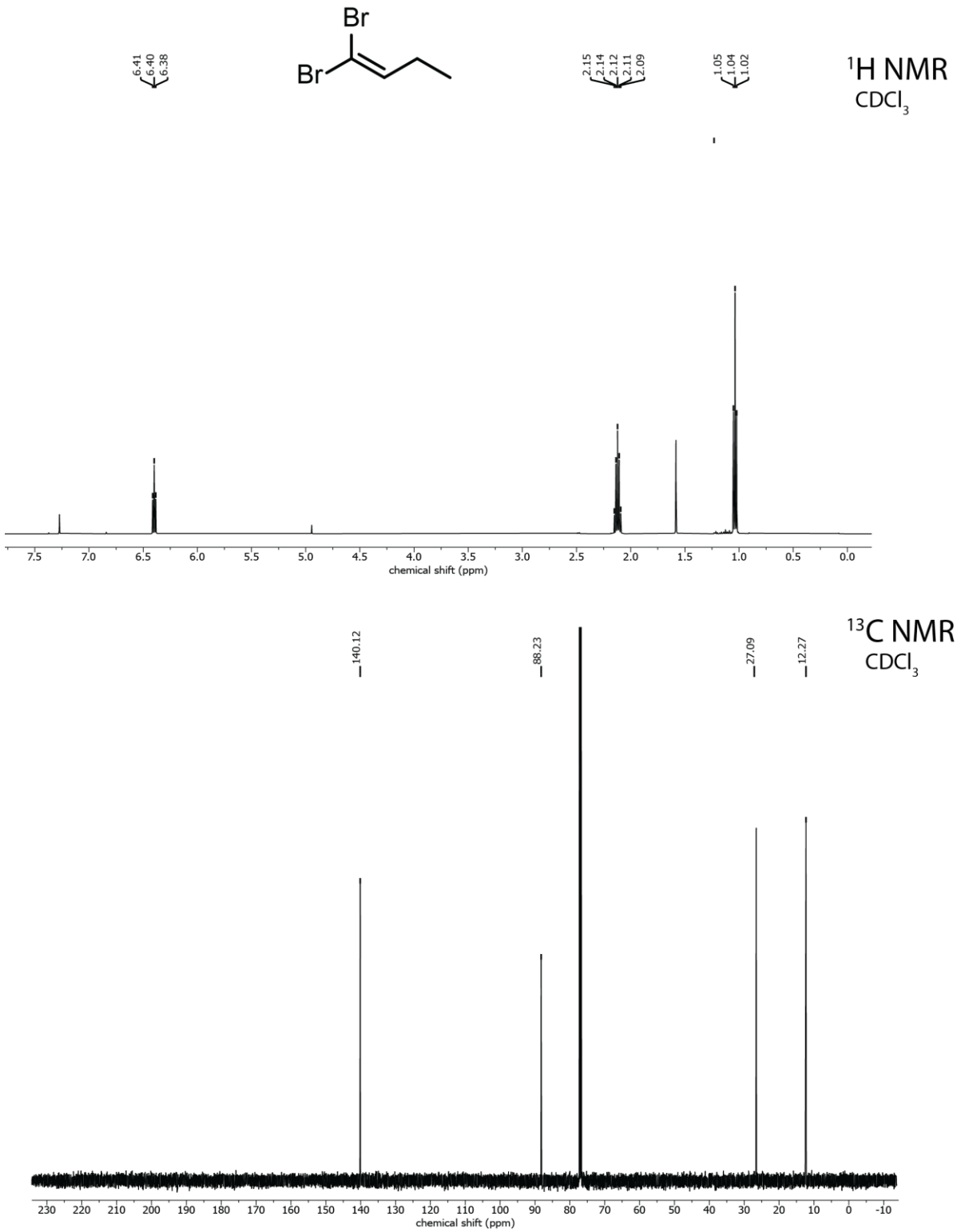

Figure S13.2. ^{1}H and ^{13}C NMR spectra of purified 1,1-dibromobutene produced by mechanochemical Wittig olefination using **1•propionaldehyde**.

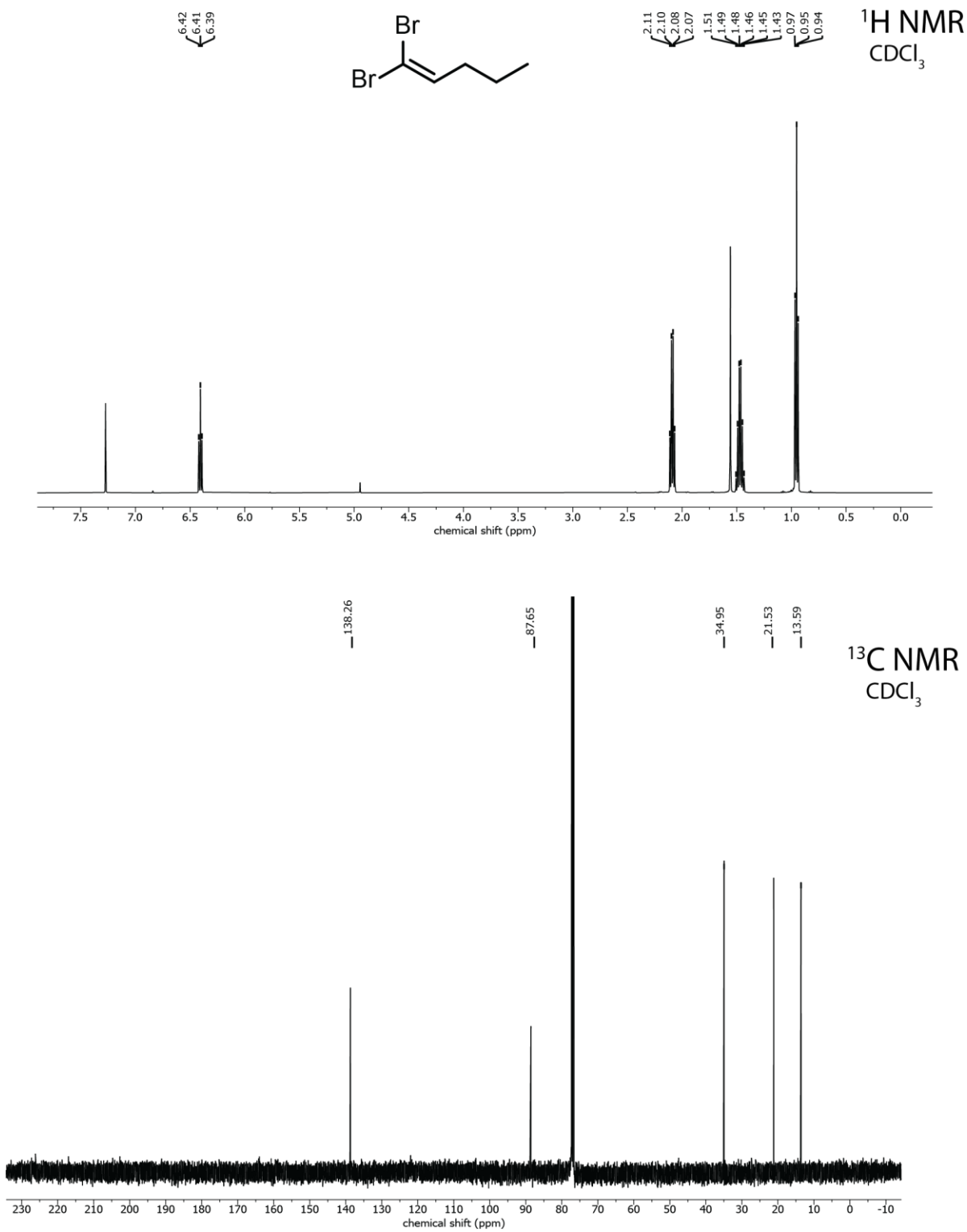

Figure S13.3. ^{1}H and ^{13}C NMR spectra of purified 1,1-dibromopentene produced by mechanochemical Wittig olefination using **1•butyraldehyde**.

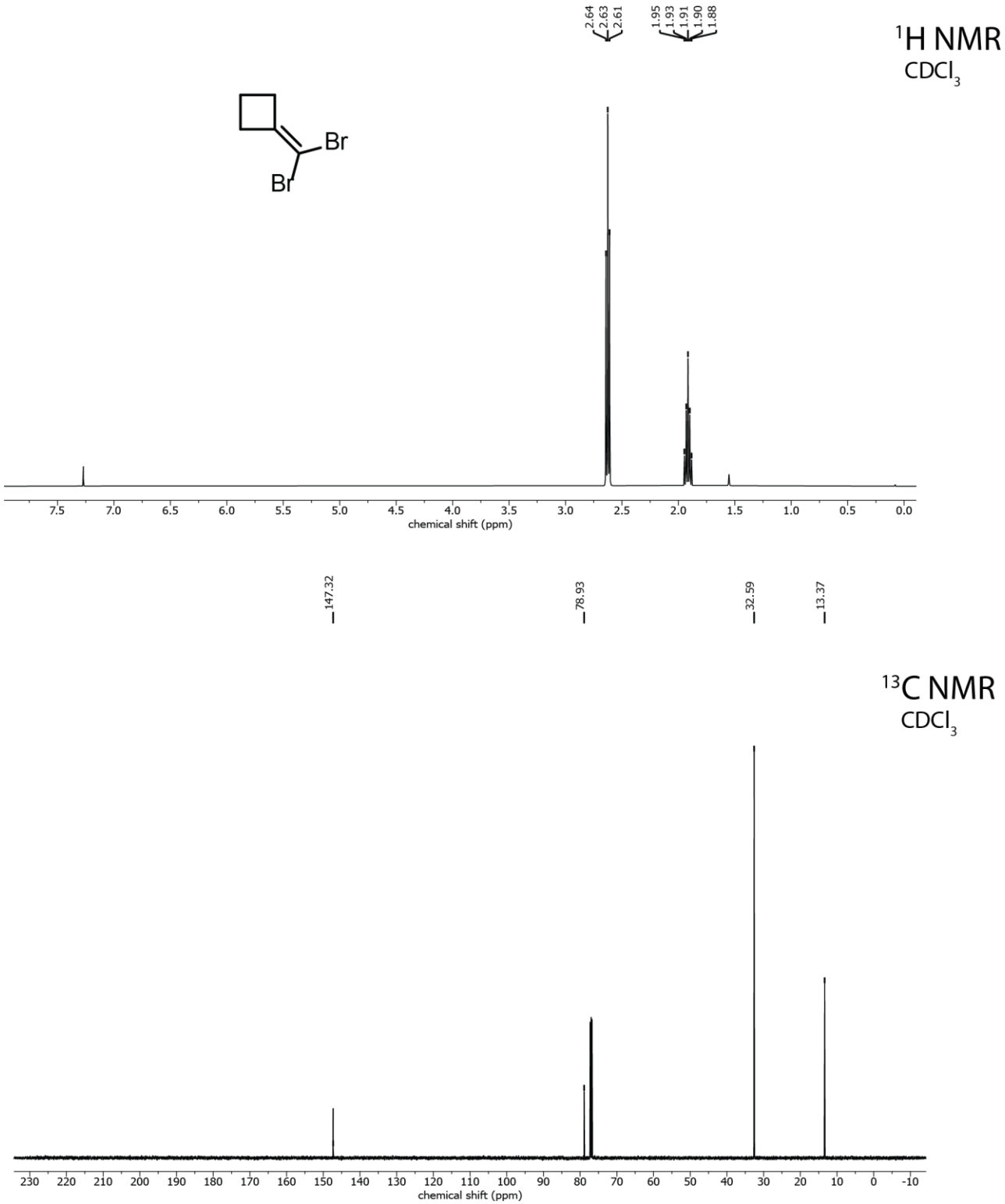

Figure S13.4. ^{1}H and ^{13}C NMR spectra of purified (dibromomethylene)cyclobutane produced by mechanochemical Wittig olefination using **1•cyclobutanone**.

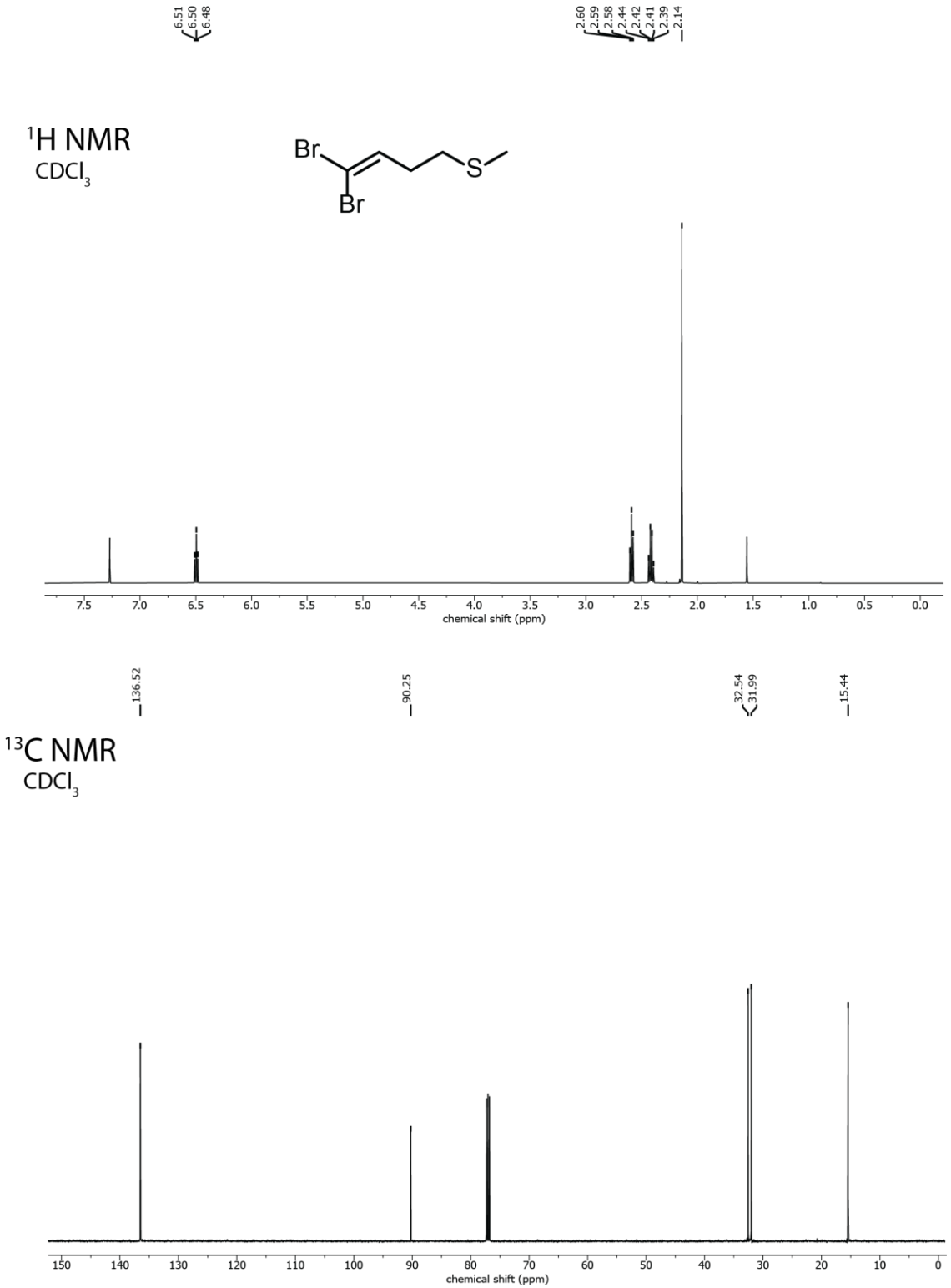

Figure S13.5. ^{1}H and ^{13}C NMR spectra of purified 1,1-dibromo-4-methylthiobutene produced by mechanochemical Wittig olefination using **1•methional**.

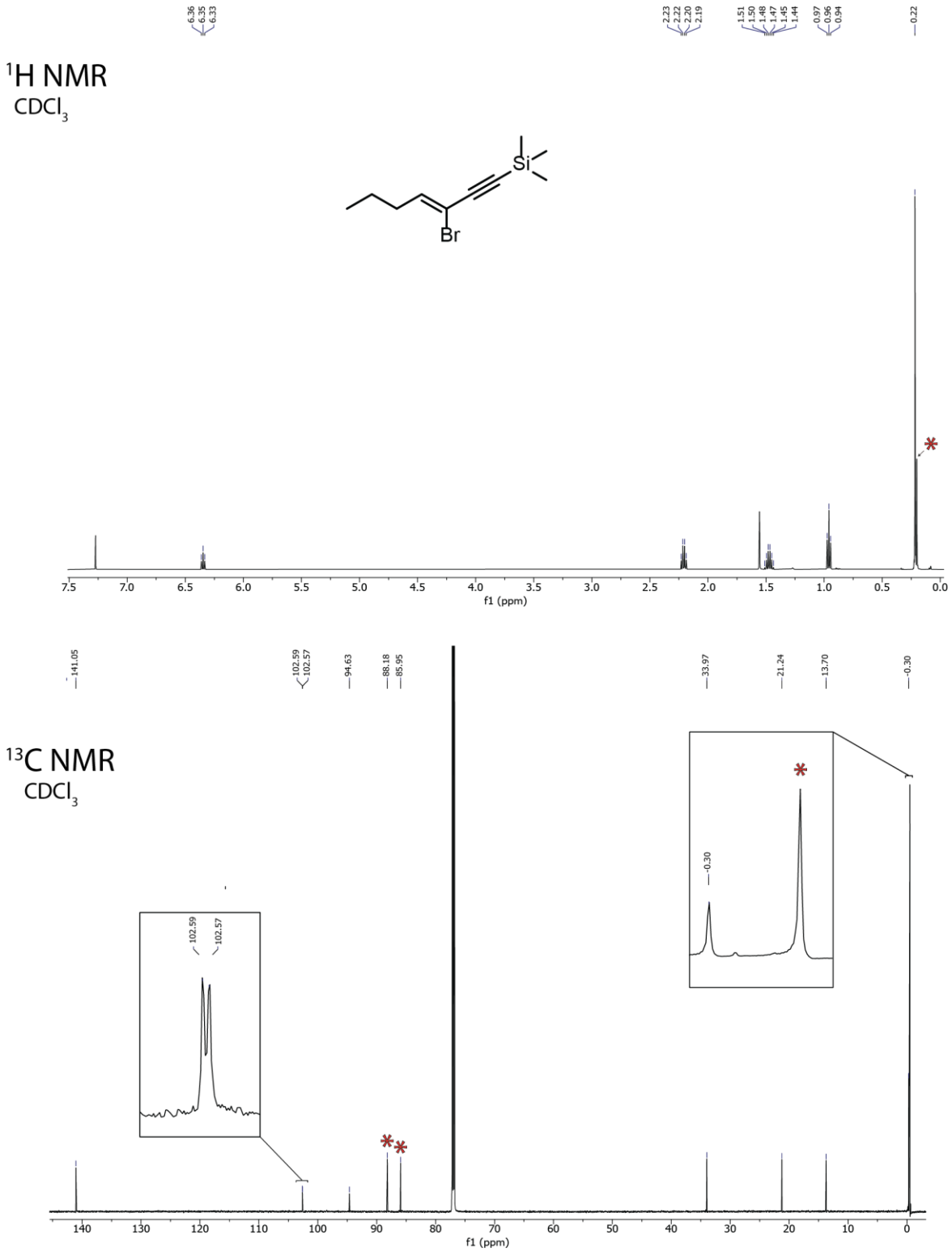

Figure S13.6. ^{1}H and ^{13}C NMR spectra of the purified eneyne Sonogashira product produced by the combined mechanochemical Wittig olefination and Sonogashira coupling using **1•butyraldehyde**. Signals of the (trimethylsiliyl)acetylene homocoupling dimer impurity are marked with "*".

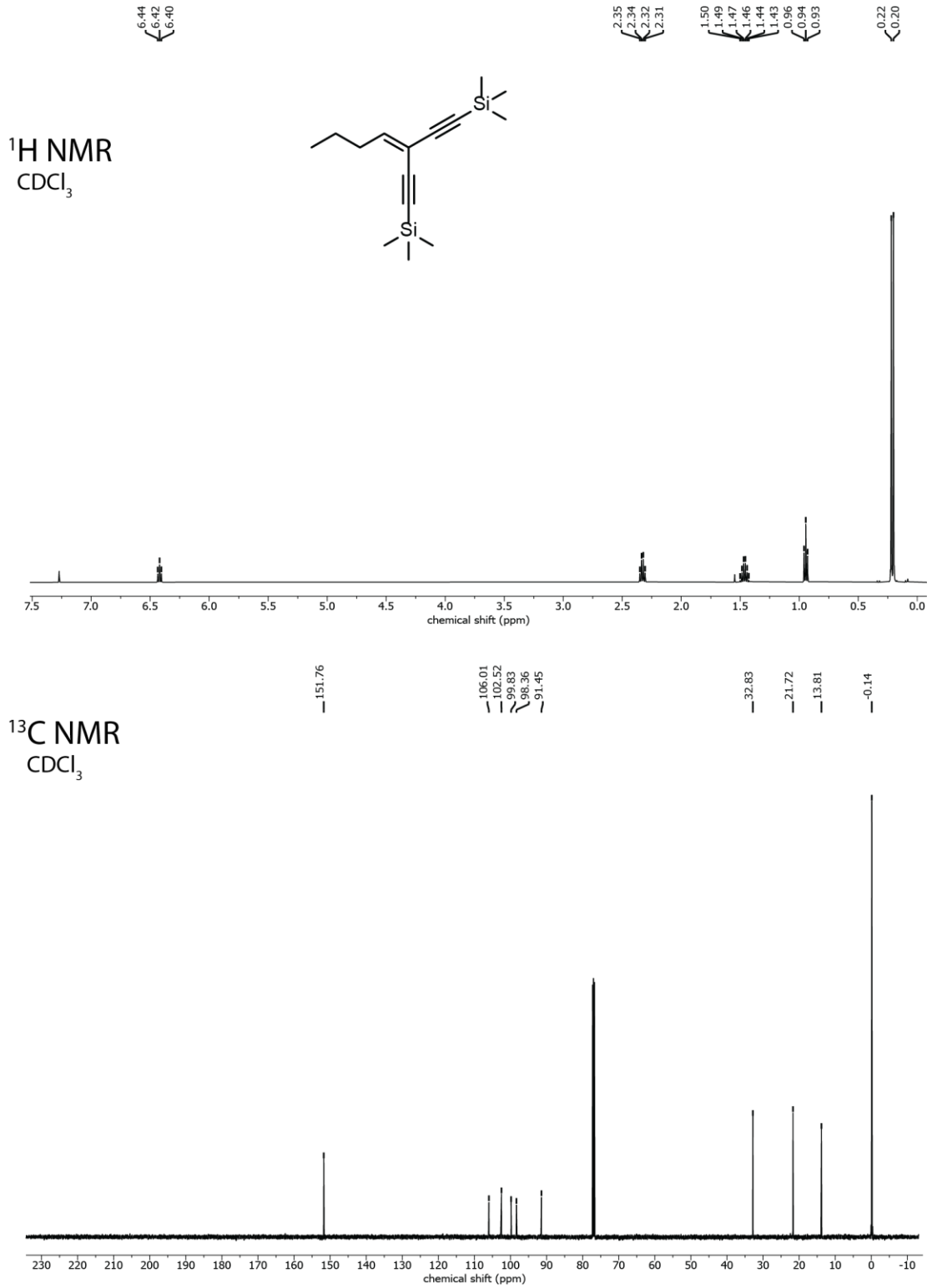

Figure S13.7. ^{1}H and ^{13}C NMR spectra of the purified enediyne Sonogashira product produced by the combined mechanochemical Wittig olefination and Sonogashira coupling using **1•butyraldehyde**.

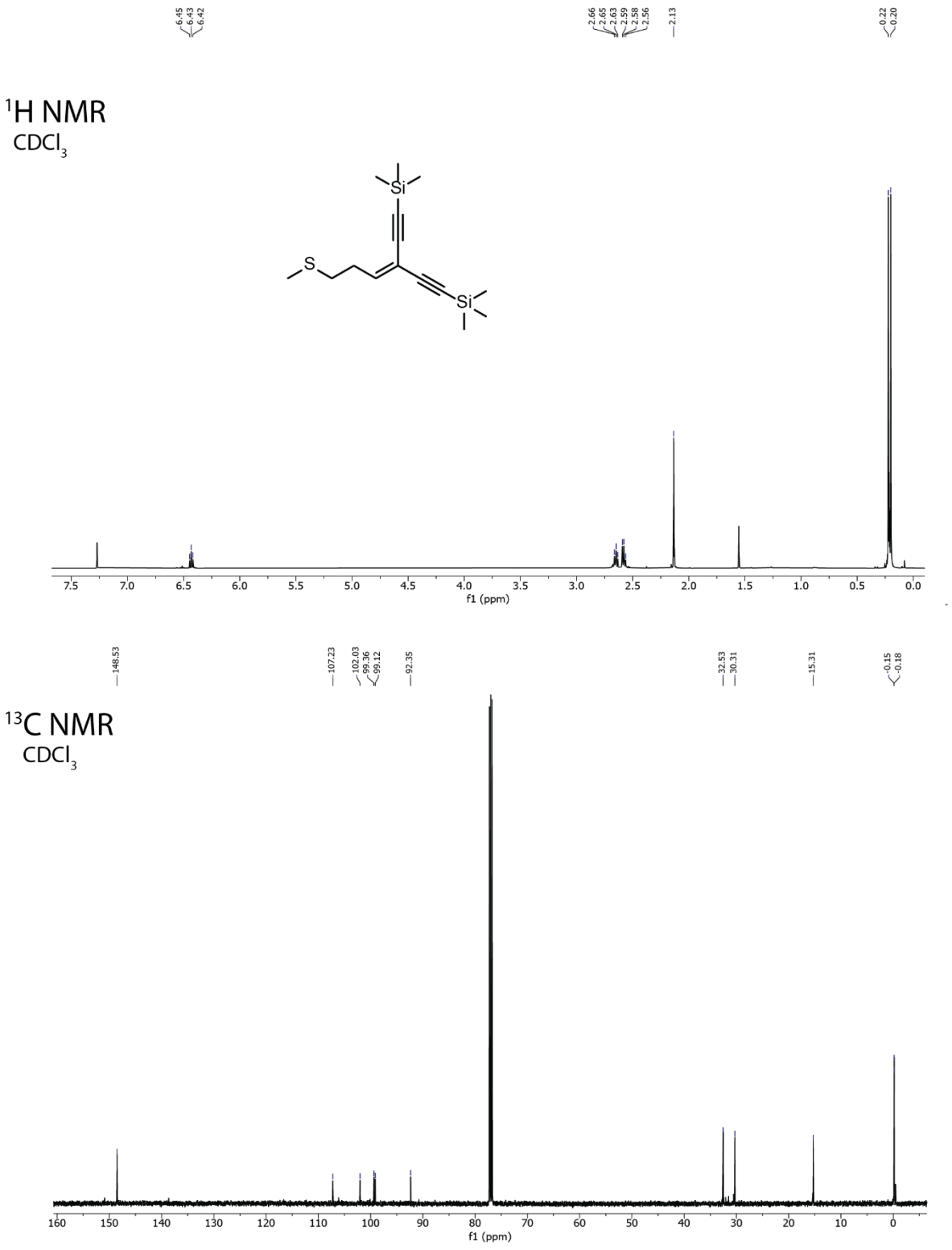

Figure S13.8. ^{1}H and ^{13}C NMR spectra of the purified enediyne Sonogashira product produced by the combined mechanochemical Wittig olefination and Sonogashira coupling using **1•methional**.

S14. References

1. P. Wolkoff, *Can. J. Chem.* **1975**, *53*, 1333-1335.
2. J. Uenishi, K. Matsui, H. Ohmiya, *J. Organomet. Chem.* **2002**, *653*, 141-149.
3. R. Appel, W. Morbach, *Synthesis* **1977,** *10*, 699-700.
4. Frisch, M. J. *et. al*., *Gaussian 16*, Revision C.01, Gaussian Inc., Wallingford, CT, **2016**.
5. a) A. D. Becke, *Phys. Rev.* **1993**, *98*, 5648-5652; b) C. Lee, W. Yang, R. G. Parr, *Phys. Rev. B* **1988**, *37*, 785-789.
6. B. P. Pritchard, D. Altarawy, B. Didier, T. D. Gibson, T. L. Windus, *J. Chem. Inf. Model.* **2019**, *59*, 4814-4820.
7. K. Momma, F. Izum, *J. Appl. Cryst.* **2011**, *44*, 1271-1276.
8. G. M. Sheldrick, *Acta Cryst.* **2015**, *A71*, 3-8.
9. G. M. Sheldrick, *Acta Cryst.* **2015**, *C71*, 3-8.
10. A. L. Spek, *Acta Cryst.* **2015**, *C71*, 9-18.
11. G. Ruban, V. Zabel, *Cryst. Struct. Commun.* **1976**, *5*, 671.
12. H. Ott, *Z. Kristallogr. Kristallgeom. Kristallphys. Kristallchem.* **1926**, *63*, 222-230.